Décomposition photocatalytique du méthanol sur des nanosphères de TiO_2 chargées de métal

Mémoire

Thuy Dung Vu

Maîtrise en génie chimique - avec mémoire
Maître ès sciences (M. Sc.)

Québec, Canada

Décomposition photocatalytique du méthanol sur des nanosphères de TiO_2 chargées de métal

Mémoire

Thuy-Dung Vu

Sous la direction de :

Prof. Maria Cornelia Iliuta, directrice de recherche

Prof. Trong-On Do, codirecteur de recherche

Résumé

L'utilisation des photocatalyseurs actifs sous iradiation solaire a attiré une attention croissante dans la création d'énergie verte et la purification de l'environnement des polluants nocifs. La photocatalyse à base de semi-conducteurs a diverses applications, notamment la décomposition des polluants organiques. En particulier, les photocatalyseurs à base de dioxyde de titane (TiO_2) sont considérés comme les matériaux les plus étudiés en raison de leur faible coût et de leurs propriétés physico-chimiques exceptionnelles. Cependant, la performance photocatalytique du TiO_2 reste encore limitée en raison de la faible absorption de la lumière et de la recombinaison rapide des porteurs de charge. Par conséquent, l'objectif principal de ce mémoire est de développer de nouvelles méthodes pour préparer des matériaux plus efficaces à base de TiO_2 pour la décomposition des polluants organiques.

Dans ce but, les nanodisques de titanate (TNDs) avec un diamètre moyen de 22 nm ont été synthétisés en utilisant différents types d'agents de coiffage, inclus l'alcool benzylique (BA), l'éther benzylique (BE) et l'oléylamine (OM). En utilisant des nanosphères de SiO_2 (SiO_2 NSs) dans le diamètre nanométrique comme noyau de la structure, les SiO_2 NSs ont été revêtus avec TNDs en utilisant une technique de dépôt couche-par-couche en présence de polyéthylène-imine (PEI) pour obtenir le TND-PEI/SiO_2 NSs. Après calcination, des TiO_2/SiO_2 NSs ayant une porosité élevée et une grande surface spécifique ont été obtenus.

Basé sur le TND-PEI/SiO_2 NSs développé, la création d'une hétérojonction entre le TiO_2 et d'autres semi-conducteurs actifs de la lumière visible est l'un des moyens intéressants de tirer profit du TiO_2 dans la région visible. Certaines solutions de cations ont été chargées sur des TND-PEI/SiO_2 NSs comme une solution de Cu^{2+}, une solution de Ni^{2+}, une solution de Pt^{2+} pour créer CuO/TiO_2/SiO_2, Ni^{2+}/TiO_2/SiO_2 et Pt^{2+}/TiO_2/SiO_2. La co-existence de CuO, Ni^{2+} et Pt^{2+} fonctionnant en tant que co-catalyseurs a considérablement amélioré la performance photocatalytique du TiO_2. Les nouveaux matériaux ont montré non seulement une grande porosité et une surface spécifique élevée, mais aussi une forte absorption de la lumière solaire. En conséquence, l'activité photocatalytique de ces

nouveaux matériaux et l'effet de différents co-catalyseurs ont été étudiés par la décomposition photocatalytique du méthanol.

De plus, le dopage est une façon bien connue et efficace pour diminuer la largeur de la bande interdite, ce qui entraîne l'absorption de plus de lumière visible par le TiO_2. Le dopage non métallique du TiO_2 a été étudié par un traitement au H_2S sur le $CuO/TiO_2/SiO_2$. La photodégradation du méthanol en solution aqueuse a été déployée pour les activités photocatalytiques du TiO_2 et a élargi son champ d'application dans le traitement de l'eau. Ces modifications ont prouvé que l'absorption de lumière par le CuO/TiO_2 est assez bonne en comparaison avec les matériaux Ni^{2+}/TiO_2 et Pt^{2+}/TiO_2. Le matériau CuO/TiO_2 après traitement au H_2S présente une performance élevée pour la dégradation du méthanol en solution aqueuse sous irradiation de lumière solaire.

Abstract

The utilization of solar light-driven photocatalysts has attracted an increasing attention in creating green energy and purifying environment from harmful pollutants. In photocatalysis technology, semiconductor-based photocatalysis has diverse applications including the decomposition of organic pollutants. In particular, titanium dioxide (TiO_2)-based photocatalysts have been extensively studied because of their low cost and outstanding physical and chemical properties. However, the photocatalytic performance of TiO_2 is not very high due to the weak light absorption and the fast charge carrier recombination. Therefore, the main target of the research presented in this thesis is to develop new methods to prepare more efficient materials based on TiO_2 for organic pollutants decomposition.

For this purpose, the uniform titanate nanodisks (TNDs) with an average diameter of 22 nm were first synthesized by using different types of capping agents, including benzyl alcohol (BA), benzyl ether (BE) and oleylamine (OM). SiO_2 nanospheres (SiO_2 NSs) in nanoscale diameter as the core of the structure were then coated with TNDs using a layer-by-layer deposition technique in the presence of polyethylenimine (PEI) solution to design the TND-PEI/SiO_2 NSs.

Based on the developed TND-PEI/SiO_2 NSs, creating a heterojunction between TiO_2 and other visible light active semiconductors is one of the interesting ways to optimize and enhance performance of TiO_2 in the visible region. In order to synthesize these TiO_2-based heterojunction composites, several cation (Cu^{2+}, Ni^{2+}, and Pt^{2+}) solutions were loaded over TND-PEI/SiO_2 NSs to obtain CuO/TiO_2/SiO_2, Ni^{2+}/TiO_2/SiO_2 or Pt^{2+}/TiO_2/SiO_2 materials, respectively. The co-existence of CuO, Ni^{2+}, and Pt^{2+} functioning as co-catalysts led to a remarkable enhancement of the photocatalytic performance of TiO_2. The new developed materials have shown not only high porosity and high specific surface area, but also strong solar light absorption. As a result, the photocatalytic activity of these new materials and the effect of different co-catalysts were investigated in the photocatalytic decomposition of methanol.

TiO_2-based heterojunction composites ($CuO/TiO_2/SiO_2$) was further treated by H_2S. This non-metal doping TiO_2 is a well-known and effective way to decrease the band gap, which can result in the absorption of more visible light. The photodegradation of methanol in aqueous solution was deployed to test the photocatalytic activities of TiO_2-based material and further widens its applications in water treatment. These modifications proved that the light absorption of CuO/TiO_2 was improved compared with Ni^{2+}/TiO_2 and Pt^{2+}/TiO_2. CuO/TiO_2 material after H_2S treatment was found to exhibit a good performance in the degradation of methanol from aqueous solutions under solar light irradiation.

Table of contents

List of figures

List of tables

Abbreviations

Ads	Adsorb
Ag	Silver
ANPOs	Advanced non-photochemical oxidation processes
AOPs	Advanced oxidation processes
Au	Gold
BA	Benzyl alcohol
BET	Braunauer-Emmer-Teller
C	Carbon
CB	Conduction band
CdS	Cadmium sulfide
CdSe	Cadmium selenide
CdTe	Cadmium telluride
CH_3OH	Methanol
Co	Cobalt
Cu	Copper
Cu_2O	Copper(I) oxide
CuO	Copper(II) oxide
CuS	Copper monosulfide
DDT	Dichlorodiphenyltrichloroethane
EDTA	Ethylenediaminetetraacetic acid
Fe	Iron
Fe_2O_3	Ferric oxide
FID	Flame ionization detector
GC	Gas chromatography
H_2O	Water
H_2O_2	Hydrogen peroxide
H_2S	Hydrogen sulfide
HCB	Hexachlorobenzene
MoS_2	Molybdenum disulfide

N_2	Nitrogen
NH_3	Ammonia
NHE	Normal hydrogen electrode
Ni	Nickel
NOMs	Natural organic matters
NPs	Nanoparticles
NSs	Nanospheres
O_2	Oxygen
O_3	Ozone
OH^-	Hydroxide ion
OH•	Hydroxyl radicals
OM	Oleylamine
P	Phosphorus
PCB	Polychlorinated biphenyl
Pd	Palladium
PEI	Polyethylenimine
POPs	Persistent organic pollutants
Pt	Platinum
ROO•	Peroxyl radical
RuO_2	Ruthenium(IV) oxide
S	Sulfur
SCE	Saturated calomel electrode
SEM	Scanning electron microscopy
SiO_2	Silica
SnO_2	Tin(IV) oxide
TB	Titanium butoxide
TCD	Thermal conductivity detector
TEA	Tetraethylammonium
TEM	Transmission electron microscopy
TEOS	Tetraethylorthosilicate
THM	Trihalomethane

TiN	Titanium nitride
TiO_2	Titanium dioxide
TiS_2	Titanium disulfide
TND	Titanate nanodisks
TR	Trap
UV	Ultraviolet spectroscopy
UV-vis	Ultraviolet-visible spectroscopy
VB	Valence band
VUV	Vacumm ultraviolet
WO_3	Tungsten trioxide
ZnO	Zinc oxide
ZnS	Zinc sulfide
ZrO_2	Zirconium dioxide

Symbols

A	Ampere
c	BET constant
d	diameter
e^-	Electron
Eg	Band gap
eV	Electron volt
kg	Kilogram
h^+	Hole
Hz	Hertz
hν	Photon energy
J	Joule
K	Kevin degree
L	Liter
m	Meter
N	Avogadro's number
$^{\circ}C$	Celsius degree
p	Equilibrium gas pressure
p_0	Saturation gas pressure
Pa	Pascal
ppm	Part per million
S	Specific surface area
V	Volt
W	Watt
λ	Wavelength
ν	Adsorbed volume of gas
ν_m	Adsorbed monolayer volume

Preface

This thesis consists of 3 sections. The first section is an introduction of the current condition of water pollution, the sustainable solar energy, as well as a brief introduction of the project which is methods of using TiO_2 material as a photocatalyst.

The second section is divided into 3 chapters. The chapter 1 is the literature review which includes three parts. The first part is an introduction of advanced oxidation processes (AOPs) which are assumed as the main factor of water pollution treatment. It contains the definition of AOPs, persistent organic pollutants (POPs) and the requirements for water cycling. The second part gives the fundamental backgrounds of photocatalyst and semiconductor including the definition of photocatalyst and mechanism. It also introduces TiO_2 as the most famous semiconductor material, its advantages and its limitations as well as the methods to overcome the limitations. The last part of this chapter introduces the objective of the project: the improvement of the phototcatalytic efficiency of TiO_2 semiconductor by controlling its morphology, coupling with other metals (Cu, Ni, Pt) as co-catalysts, and doping TiO_2 with non-metal elements.

Chapter 2 describes the methodology, synthesis of the materials, characterization techniques and photocatalyst efficiency tests.

Chapter 3 concerns the results and discuss the effect of the structure of TiO_2, the concentration of metal loading and the effect of different metals and non-metal elements.

Finally, the third section summarizes the main findings of this research, the general conclusions and the recommendations for future work.

Acknowledgements

Firstly, I would like to thank Professor Maria Cornelia Iliuta for her supervision and guidance, support and patience throughout my Master studies, as well as for the great opportunity that she offered me to work in her lab during the last two years. I would also like to thank my co-director, Professor Trong-On Do who gave me invaluable thoughtful insights, advice, supports, discussions, and encouragements.

I am also very grateful for the generous and contentious help from present and former members of professors Iliuta and professors Do research groups at the Department of Chemical Engineering, Université Laval.

Finally, Finally, I am grateful to my directors (professors Iliuta and Do), as well as to the agreement between the Governments of Québec and Vietnam, for the financial support.

Most important of all, especially I would like to thank my parents and my sister.

Finally, I would like to express my gratitude to all my Vietnamese friends at Laval University for their friendship, supports, and encouragements.

Introduction

Water is an essential element for existence, but the increasing demand and shortage of clean water sources due to the rapid improvement of industrialization, population growth, and global warming have ended up a serious problem of environmental pollution in the world. It is assessed that about 4 billion people around the world experience to have no or little access to clean and sanitized water supply, and millions of people died of severe water-related diseases every year [1]. At the same time, the expanding water contamination due to the overwhelming discharge of micro-pollutants and contaminants into the natural water cycle [2,3] may lead these statistical figures growing in the short future. Therefore, many strategies and solutions have been adopted to yield clean and clear water resources. Therefore, the development of advanced with low-cost and high efficiency water treatment technologies to treat the wastewater is highly needed. Several methods have been employed for water treatment, such as methods using activated carbon adsorption, chemical oxidation, or biological treatment etc. Even they have certain practical applications, all those methods are either slow or non-destructive for some more persistent organic pollutants [4].

Besides water, light from sun or solar energy is another important element for life. It helps the creature grow, makes us able to see objects around, and maintains the temperature on the earth. Solar energy, together with energies from wind, geothermal, hydropower, bio-fuel and biomass, are called renewable energies. Among them, solar energy is the ultimate renewable source to sustain all lives on earth and the most abundant source of energy on our planet, which provides about 23000 TW power every year, hundreds times higher energy potential than other traditional energy sources (such as coal, petroleum, nature gas,..) (as shown in **Figure I.1)** [5]. That's why currently the usage of solar energy with new materials is attracted a lot of attention in improving water treatment process.

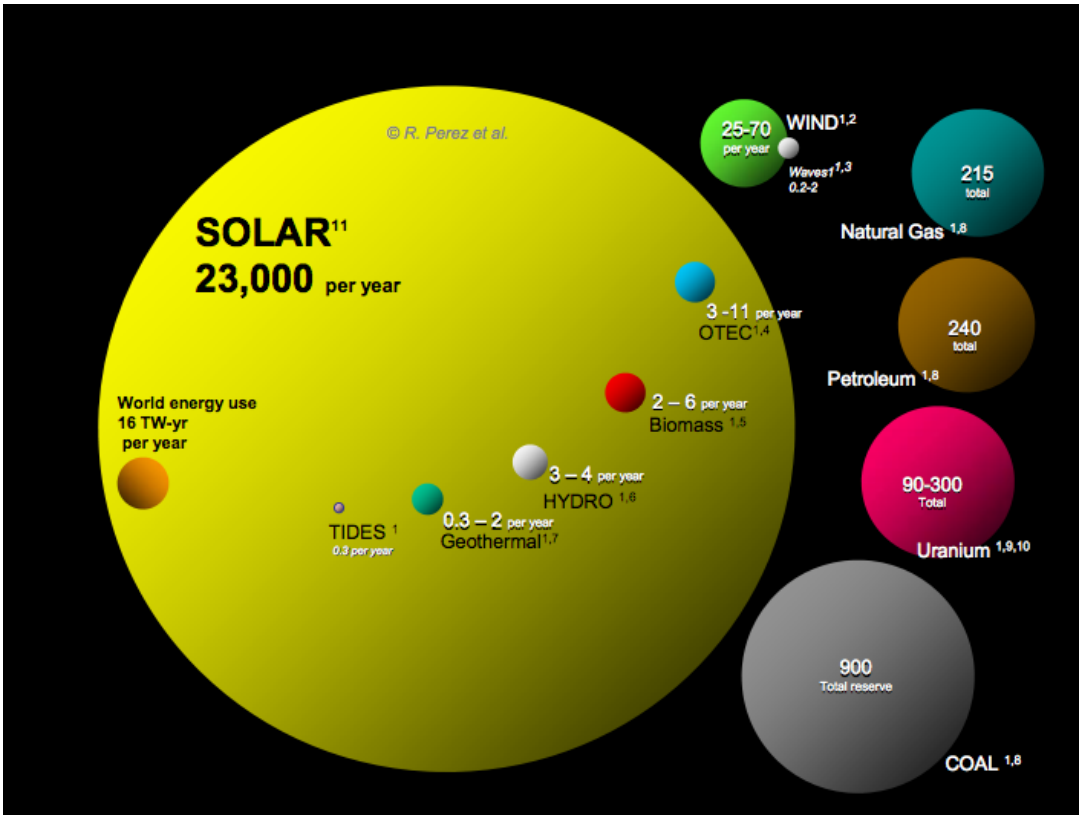

Figure I.1: Global energy potential (Terawatt/years) [5].

In particular, the usage of solar energy in waste water treatment using photocatalytic process is the most sustainable development, and meets many standards of characteristics of green science [6]. Moreover, variety of important features for the heterogeneous photocatalysis have extended their attainable applications in water treatment, such as: ambient operating temperature and pressure [7], complete mineralization compounds without secondary pollution [8] and low operating costs [4]. However, it has a big challenge related to efficiency in harvesting, converting, and storing solar energy, therefore, the development of photocatalysis using semiconductors has been considered as the promising solutions for pollution treatment.

Recently, many studies have been focused on the development of sunlight-driven photocatalysts using semiconductors such as TiO_2 [9], ZnO [10], Fe_2O_3 [11], CdS [12] and ZnS [13], etc. All of them demonstrated their efficiency in degrading a wide range of organic materials into readily biodegradable compounds, and eventually mineralized them

to water [14]. However, these semiconductor materials still suffer from two weaknesses: weak photon absorption and poor electron-hole pair separation. Therefore, the development of highly efficient photocatalysts that absorb a large amount of solar energy and exhibit high charge separation is a key requirement for the conversion of solar radiation into chemical energy.

Among the semiconductor catalysts, titanium dioxide (TiO_2) has received the greatest interest in photocatalysis. The TiO_2 is one of the most active photocatalyst semiconductors under the photon energy of 300 nm < λ < 390 nm and remains stable after many catalytic cycles [1]. More than these, the variety functional properties of TiO_2 catalyst such as their chemical and thermal stability, resistance to chemical breakdown and their strong mechanical properties have provided its wide application in photocatalytic water treatment. Moreover, TiO_2 nanoparticles (NPs) are easily produced, inexpensive and showed good stability under illumination in most environment conditions. However, like any other semiconductor materials, TiO_2 with the intrinsic wide band gap energy of 3.2 eV for anatase phase, TiO_2 absorbs only a small fraction of solar light (less than 5% of solar energy is emitted as UV irradiation) [15]. This reason causes the major drawback limits of TiO_2 in large scale applications. To improve the performance of TiO_2, a significant part of research on TiO_2 has been performed, and a number of reviews on various aspects of TiO_2 have been published to understand and improve the performance of TiO_2 as well as TiO_2-based materials.

As an objective to improve performance of photocatalyst in waste water treatment, in my thesis, I focused on enhancing the photocatalytic performances of TiO_2 semiconductor as a catalyst, which includes improving three crucial factors: i) charge separation by employing co-catalysts; ii) surface area by controlling the morphology; and iii) light absorption by coupling with non-metals materials. Using SiO_2 spheres as the platform, the prepared TiO_2-based material can exhibit great photocatalytic performances towards organic pollutant degradation under sunlight irradiation.

Chapter 1: Literature review

1.1. Organic pollutants and advanced oxidation processes

1.1.1. Persistent organic pollutants

Pesticides, herbicides, and fungicides are toxic chemicals, which persist for long periods of time in the environment due to their stability and low decomposition rates [16,17]. In countries where the economy is based primarily on agriculture, the amount of chemicals used for plant protection is increasing, so the number of chemicals which dissolve in water, soak up the soil, enter the surface water, rivers, lakes, and ponds, is spreading in underground waterways, and accumulating more and more. Among these, the most notable are persistent organic pollutants (POPs) which are defined as "chemical substances that persist in the environment, bioaccumulate through the food web, and pose a risk of causing adverse effects to human health and the environment" [18]. These substances have a great impact on human health and ecology, causing cancer, neurological damage, reproductive disorders, teratogenicity, immune system degradation, and death. These substances are non-decomposable in the environment over time, can move from region to region, and spread very far away. They are the subject of the Stockholm International Convention, which has been signed by 151 countries [18,19], committed to eliminating production and use of intentionally produced POPs, eliminate unintentionally produced POPs where feasible, and manage and dispose of POPs wastes in an environmentally sound manner. The Stockholm Convention identifies the substances in three different categories (**Table 1.1)** [20].

Due to the harmful consequences of the organic pollution, in general, which affects the habitat and the health of the community, the list of pollutants is nowadays expanded [21]. Thus, we need to understand and control the wide-spread environmental pollution of POPs and also find the strategies to reduce the harmful of POPs on environment. Current studies aimed at minimizing POPs in the environment are investigating their behavior in photocatalytic oxidation reactions [22] or using semiconductor materials in photocatalytic reactions to adsorb or to decompose POPs [23].

Table 1.1: Distinct substances listed in three categories [20].

Categories	Substances
A. Elimination	Pesticides: aldrin, chlordane, dieldrin, endrin, heptachlor, hexachlorobenzene (HCB), mirex, and toxaphene. Industrial chemicals: polychlorinated biphenyls (PCBs) and HCB which also has uses in industrial chemicals
B. Restriction	Dichlorodiphenyltrichloroethane (DDT) which can only be used for disease vector control in accordance with World Health Organization recommendations
C. Unintentional Production	Polychlorinated dibenzo-p-dioxins ("dioxins") and polychlorinated dibenzofurans. Also PCB and HCB are covered as unintentional byproducts.

1.1.2. Sterilization requirements for drinking water and domestic water

In addition to the persistent organic and toxic substances mentioned above, nature water usually contains natural organic matter (NOM) such as humic acids, organic soluble acids, proteins, lipids, hydrocarbons, and amino acids [24–26]. Their type and amount in the nature water vary according to the sources of water and the region. As a result, to reach the demand of clean water to meet the living needs and standards, NOM will be combined with the chlorine in the treatment of surface water to produce clean water for drinking and other needs of life [23,27,28]. However, in chlorination water purification process, there are other byproducts, mainly chlorine containing organic substances, such as trihalomethane (THM), including trichloromethane (chloroform), dibromochloromethane, bromodichloromethane and tribromomethane (bromoform). These compounds, particularly chloroform, will cause damage to the liver, kidneys and have been proven to be related to the cause of cancer (due to the International Agency for Research on Cancer - IARC) [29]. Therefore, the addition of decomposition NOMs process before chlorination for

sterilization helps to minimize the usage of chlorine in natural water treatment as well as to reduce their harms to human health.

1.1.3. Water recycling requirements

According to scientists, the world in 2030 will suffer from lacking of water [30]. Therefore, it is important to have effective technologies that thoroughly treat contaminants in water, especially POPs and NOMs, in order to recover clean water from different sources. Traditional technologies (e.g. chlorination) do not allow to solve these problems, therefore, there are opportunities and challenges in the research related to advanced technologies for wastewater treatment to support traditional technologies in solving these problems. There are some highlights in advanced technologies applied in water and wastewater treatment technologies:

- Membrane filtration technologies
- Ultraviolet irradiation disinfection
- Advanced oxidation processes – AOPs

Three technologies above are applied in water treatment including the removal of fine particles, bacteria, colloids, viruses, NOMs, POPs, etc. However, membrane filtration technologies have some disadvantages such as high cost and mechanical fragility have hindered their widespread use [31]. Ultraviolet (UV) irradiation disinfection also has some drawback such as UV disinfection is not cost-effective; UV disinfection with low-pressure lamps is not effective with total suspended solids levels above 30 mg/L [32] and UV water treatment is strongly depended on the flow rate — if the flow is too high, water will pass through without sufficient UV exposure, if the flow is too low, heat may build up and damage the UV lamp [33]. On the other side, the AOPs technology is called water treatment processes of the 21st century due to its high efficiency for degradation of organic pollutants.

1.1.4. Advanced oxidation processes

Advanced oxidation processes (AOPs) developed for potable water treatment in the 1980s, which are defined as the oxidation processes involving the generation of hydroxyl radicals (OH•) in sufficient quantity to affect water purification [34,35]. In general, AOPs are the processes based on the production of very highly reactive transitory species (i.e. H_2O_2, OH^-, O_3 or irradiation) [4,35,36]. When AOPs are applied for wastewater treatment, hydroxyl radicals generated by AOPs tend to interact with the organic matter through three main mechanisms: (i) hydrogen abstraction from aliphatic carbon atoms yielding carbon-centered radicals, (ii) electrophilic addition to double bonds or aromatic rings, and (iii) electron transfer reactions, where OH• gains an electron from an organic substituent [37,38]. Thus, they are expected to sufficiently destruct wastewater pollutants, mineralization of organic compounds, water pathogens, and disinfection byproducts, therefore, providing an ultimate solution for wastewater treatment [39]. Several methods are available for generating OH• radicals:

- Advanced Non-Photochemical Oxidation Processes – ANPOs: generate hydroxyl radicals without using light energy.
- Advanced Photochemical Oxidation Processes – APOs: generate hydroxyl radicals using light energy.

Hydroxyl radical generation mechanisms are briefly summarized in **Table 1.2**.

Table 1.2: Hydroxyl radical generation mechanisms.

No.	Elements	Specific reaction	Name of process
1	H_2O_2/Fe^{2+}	$H_2O_2 + Fe^{2+} \rightarrow Fe^{3+} + OH^- + OH\bullet$	Fenton
2	H_2O_2/Fe^{2+}(ion)/hv	Fe^{3+} (ion) + $H_2O \rightarrow Fe^{2+} + H^+ + OH\bullet$ (hv) $H_2O_2 + Fe^{2+} \rightarrow Fe^{3+} + OH^- + OH\bullet$	Photo-Fenton
3	H_2O_2/Fe^{3+}/hv	$Fe^{3+} \rightarrow Fe^{2+}$ + R (hv) λ = 300 - 500 nm $H_2O_2 + Fe^{2+} \rightarrow Fe^{3+} + OH^- + OH\bullet$	Modified Photo-Fenton
4	H_2O/ anode Fe/ electricity	$O_2 + 2\ H_2O \rightarrow 4\ OH\bullet$ (Electricity)	Electrochemical Fenton
5	H_2O_2/O_3	$H_2O_2 + 2\ O_3 \rightarrow 2\ OH\bullet + 3\ O_2$	Peroxone
6	O_3/ reactant	$3\ O_3 + H_2O \rightarrow 2\ OH\bullet + 4\ O_2$ (with reactant)	Catazone
7	H_2O/ electricity	$H_2O \rightarrow H\bullet + OH\bullet$ (Electricity)	Electrochemical Oxidation
8	H_2O/ High energy	$H_2O \rightarrow H\bullet + OH\bullet$ (20 - 40 kHz)	Ultrasound
9	H_2O_2/UV	$H_2O_2 \rightarrow 2\ OH\bullet$ (λ = 220 nm)	UV/Oxidation
10	O_3/UV	$O_3 + H_2O_2 \rightarrow 2\ OH\bullet + O_2$($\lambda$ = 253,7 nm)	UV/Oxidation
11	H_2O_2/O_3/UV	$H_2O_2 + O_3 + H_2O \rightarrow 4\ OH\bullet + O_2$ (λ = 253,7 nm)	UV/Oxidation
12	H_2O/Vacuum UV (VUV)	$H_2O \rightarrow H\bullet + OH\bullet$ (With VUV) (λ < 190 nm)	VUV/Oxidation

13	TiO_2/ UV	$TiO_2 \rightarrow e^- + h^+$ ($\lambda > 187.5$ nm) $h^+ + H_2O \rightarrow H^+ + OH\bullet$ $h^+ + OH^- \rightarrow H^+ + OH\bullet$	Semiconductor Photocatalytic

Hydroxyl radicals are the powerful oxidizing agents. The OH• radical is the most reactive oxidizing agent in water treatment, with an oxidation potential between 2.8 eV (pH = 0) and 1.95 eV (pH = 14) vs. SCE (saturated calomel electrode, the most commonly used reference electrode) [40]. It is very non-selective and reacts rapidly with different elements with the rate constants of 10^8 - 10^{10} $M^{-1}s^{-1}$. Hydroxyl radicals attack organic pollutants through four basic pathways: radical addition, hydrogen abstraction, electron transfer, and radical combination [41]. Their reactions with organic compounds produce carbon-centered radicals (R• or R•–OH). In the presence of O_2, these carbon-center radicals may be transformed into organic peroxyl radicals (ROO•). All these radicals further react to form more reactive species such as H_2O_2 and $O_2\bullet-$, leading to chemical degradation and even mineralization of these organic compounds. Because hydroxyl radicals have a very short lifetime, they are only in-situ produced during different processes, including a combination of oxidizing agents (such as H_2O_2 and O_3), irradiation (such as ultraviolet light or ultrasound), and catalysts (such as Fe^{2+}) [39]. Example of organic compounds oxidized by OH• radicals are given in **Table 1.3** [42].

In ANPOs process, although H_2O_2 is a strong oxidant, its single application for wastewater treatment is not efficient to remove many organic compounds, including NOM, due to the kinetic limitations at conventionally applied peroxide concentration [43]; ozone utilization to remove NOM is highly depending on the reaction pH and usually leads to the formation of aldehydes and carboxylic acids, which do not react with ozone which tends to limit the efficiency of the ozonation process [44].

Table 1.3: Examples of organic compounds oxidized by OH• radicals [42].

Group	Organic compounds
Acid	formic, gluconic, lactic, malic, propionic, tactaric
Alcohol	benzyl, tert-butul, ethenol, ethylene glycol, glycerol, isopropanol, methanol, propenediol
Aldehyde	acetaldehyde, benzaldehyde, formaldehyde, glyoxal, isobutylraldehyde, trichloroecethaldehyde
Aromatic	benzene, chlorobenzene, chlorophenol, creozot, dichlorophenol, hydroquinon, p-nitrophenol, phenol, toluene, trichlorophenol, xylene, trinitrotoluene
Amine	anilin, diethylamin, dimethylamin, dimethylformamic, EDTA, propandiamin, n-propylamin
Dye	antraquinon, diazo, monoazo
Ester	Tetrahydrofuran
Ketone	dihydroxyacetone, methyl-ethyl-ketone

Comparing with ANPOs process, in APOs process, the heterogeneous photocatalytic oxidation is based on the utilization of UV radiation to photoexcite semiconductor catalysts to attack organic compounds in water for purification purposes. Various photocatalysts such as ZnO [10], Fe_2O_3 [11], CdS [12], Cu_2O [45], etc were successfully applied to degrade a wide array of recalcitrant organic compounds into easily biodegradable ones [46,47]. Furthermore, the primary source of APOs is UV radiation that can be obtained from sunlight, APOs are highly valued by researchers in the field of solving environmental problems. This thesis will focus primarily on APOs process, using light to decompose organic pollutants that causing the water pollution.

1.2. Generalities on photocatalyst and semiconductor

In early 1901, G. Ciamician was one of the first chemists to conduct experiments to study whether light would enable chemical reactions [48]. In 1911, the term "photocatalyst" was first appeared in several research to refer to the reactions occurring under the simultaneous action of the catalyst and the light ("photo") [49]. In other words, the photocatalysis is a process which uses light to activate a substance which modifies the rate of a chemical reaction without being involved itself. Nowadays, the term "photocatalyst using semiconductor" becomes a key solution for energy production and pollutant degradation with several characteristics out of 12 principles of green chemistry [6], including:

- The use of greener safer photocatalyst, low cost, and chemical stability.
- The use of mild oxidants, such as molecular oxygen.
- The possibility to work with mild reaction conditions running closer to room temperature and pressure.
- The requirement of very few auxiliary additives.
- No harmful chemical productions.
- The use of eternally energy resources (solar energy).
- The catalysts can be recovered and reused.

In the end of the 1960s, Fujishima et al. [50] first succeeded the project using n-type TiO_2 as semiconductor electrode to investigate the photoelectrolysis of water, marked a turning point in the history of science and technology. The semiconductor is a solid state matter that has the conductivity between the conductor and the insulator, depending the conditions, it can conduct electricity or not. The semiconductors can be classified into two types: n-type semiconductor and p-type semiconductor. In many researches, semiconductor materials like TiO_2, ZnO, Fe_2O_3, CdS, and ZnS demonstrated their efficiency in degrading a wide range of organic materials into readily biodegradable compounds, and eventually mineralized them to water [14].

1.2.1. What is photocatalyst

Among the renewable energy resources, the solar energy, which is green and free, is the most interesting, the ideal energy source for overcoming the current environmental problems. Since Fujishima and Honda first reported the generation of H_2 and O_2 through the photo-electrochemical splitting of water on TiO_2 in 1972 [50], the photocatalytic properties of certain materials have been used to convert solar energy into chemical energy to oxidize or reduce materials to obtain useful materials, and to remove pollutants and bacteria [50–54].

1.2.1.1. Valence band, conduction band and band gap

The electronic structure of a semiconductor includes 3 regions (**Figure 1.1**):

- **Valance band** (VB): The lowest energy region in the energy scale, where electrons are strongly bonded to the atom and are not flexible.
- **Conduction band** (CB): The highest energy region in the energy scale, where the electrons are mobile and flexible which will conduct electricity when electrons are present. The electric conductivity increases when the electron density increases.
- **Forbidden band**: The area between the valence band and the conduction band, where is no energy so electrons cannot exist in the forbidden band. The distance between the bottom of the CB and the top of the VB is called the band gap.

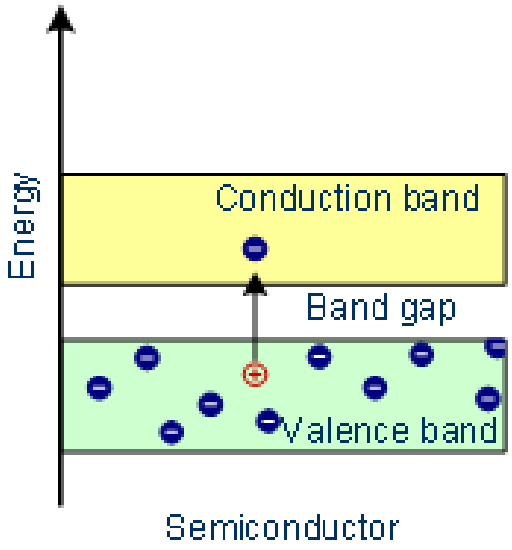

Figure 1.1: Electronic regions of a semiconductor material.

1.2.1.2. Electron trap

The semiconductor with a wide band gap (Eg > 3 eV) can only absorb UV light, which accounts for only 5% of solar energy. A narrow band gap semiconductor (Eg < 3 eV) can be activated by visible light irradiation, which constitutes 43% of the sunlight spectrum [55,56]. **Figure 1.2** shows some examples of the band gaps various semiconductors (E is the energy and NHE is normal hydrogen electrode).

For semiconductor materials with Eg < 3.5 eV (such as TiO_2 (Eg = 3.2 eV), WO_3 (Eg = 2.8 eV), CdS (Eg = 2.5 eV), ZnO (Eg = 3.2 eV),…), if the electrons in the VB are stimulated by photon energy greater than the band-gap energy of the material, therefore, the electron (e^-) of VB is excited, they can cross the forbidden band to the CB and leave a hole (h^+) in the VB becoming the conditionally conductive, used for photocatalyst [15].

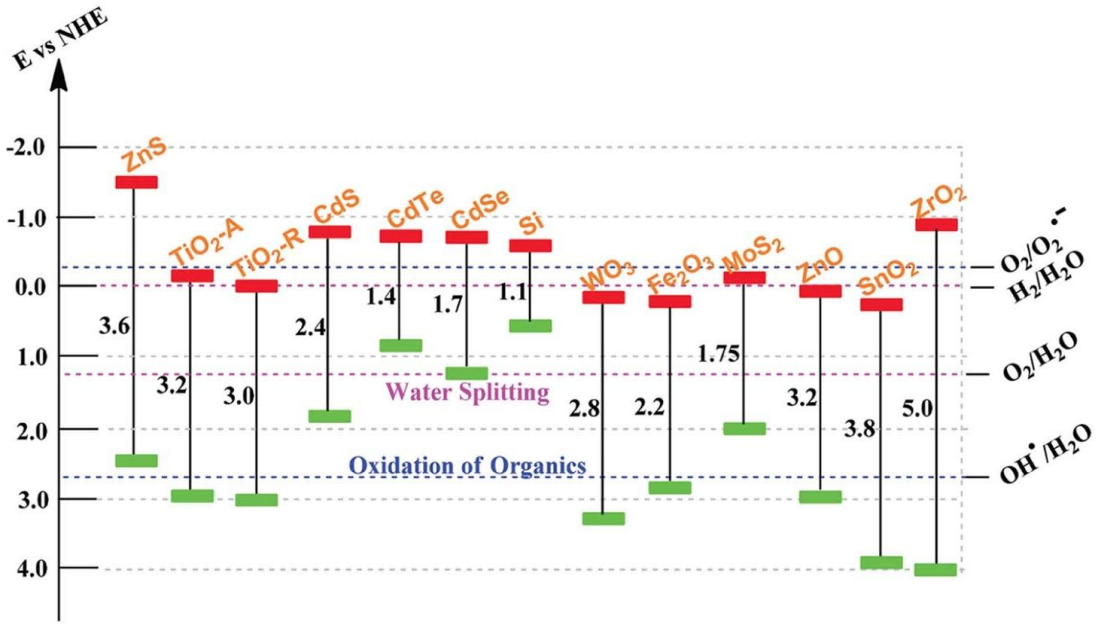

Figure 1.2: Band gap of various semiconductors [57].

With the existence of semiconductor (e.g. TiO_2), after being illuminated by the light source with higher energy than the band gap, the electron (e^-) is excited to the CB, leaving behind a hole (h^+) in the VB then the charge carriers migrate it to the photocatalyst surface. The carriers can recombine at a surface trap (**Figure 1.3** (3) and Eq. 1) or in the bulk (**Figure 1.3** (4) and Eq. 4); otherwise, they can interact with acceptor (A) (**Figure 1.3** (1) and Eq. 2) or donor (D) (**Figure 1.3** (2) and Eq. 3) species adsorbed on the surface. Therefore, it is widely accepted that the greater the number of photo-generated carriers that are generated and reach the surface, the more efficiently the photoactive material will perform, and thus, photocatalytic performance is significantly influenced by the incident light absorption ability and charge separation efficiency of the catalyst.

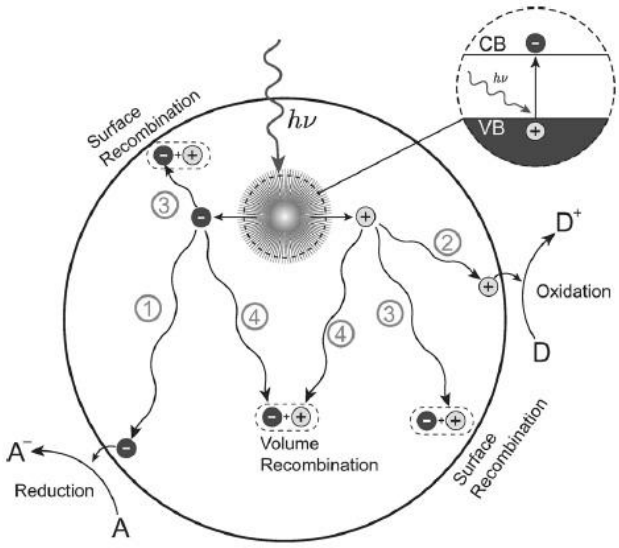

Figure 1.3: General processes in a semiconductor photocatalyst [58].

The series of chain oxidative-reductive reactions [58]:

Excitation of the catalyst:	Semiconductor + hv→ e^- + h^+	(1)
Charge – carrier trapping of e^-:	e^-_{CB} → e^-_{TR}	(2)
Charge – carrier trapping of h^+:	h^+_{VB} → h^+_{TR}	(3)
Electron-hole recombination:	e^-_{TR} + h^+_{VB}(h^+_{TR}) → e^-_{CB} + heat	(4)

1.2.2. Titanium dioxide material

1.2.2.1. Physical properties

Titanium dioxide (TiO_2) is odorless white and tasteless powder. Its density 3.83-4.24 g/cm^3 and the melting point is 1870 $^{\circ}$C. TiO_2 is insoluble in water, but soluble in hot concentrated sulfuric acid, hydrofluoric acid. TiO_2 belongs to the family of transition metal oxides and exists in three different crystal forms: anatase (tetragonal), rutile (tetragonal), and brookite (orthorhombic) [59]. **Table 1.4** and **Figure 1.4** show the physical properties and the crystalline structure of three different crystal forms of TiO_2.

Table 1.4: Physical properties of three different crystal forms of TiO_2 [59].

Properties	Crystalline forms		
	Anatase	Rutile	Brookite
Crystalline Structure	tetragonal	tetragonal	orthorhombic
Lattice Constants	a=b=0.3733 c=0.9370	a=b=0.4584 c=0.2953	a=0.5436 b=0.9166 c=0.5135
Density (g/cm^3)	3.83	4.24	4.17
Melting point ($^{\circ}C$)	Turning to rutile	1870	Turning to rutile
Boiling point ($^{\circ}C$)	2927	-	-
Band gap (eV)	3.2	3.0	-

Anatase and rutile are the most studied forms of nanostructured TiO_2. In fundamental studies, the rutile TiO_2 is the most explored, whereas the anatase TiO_2 is the most investigated form in the applied studies [15]. Heat treatment has a vital role in the synthesis of particles, affecting morphology, crystallinity, and porosity, and causing a decline in the surface area. Upon heating, the TiO_2 anatase and brookite can be transformed into rutile (**Table 1.4**). Anatase form can be easily synthesized at the lower temperature (below 400 ºC), whereas rutile form is frequently synthesized at moderate temperature (from 400 to 600 ºC) [60]. Rutile TiO_2 has a tetragonal structure and contains 6 atoms per unit cell. Most researchers in the field argue that rutile is the most stable phase at high temperature and pressure, up to 60 kbar [61]. Anatase and brookite transform to the rutile phase after reaching a certain particle size, the rutile phase becoming more stable than anatase for particle sizes larger than 14 nm [62]. When compared with the rutile phase, anatase also has a tetragonal structure but the distortion of the TiO_6 octahedron is slightly larger. It is more stable than the rutile at 0 K, but the energy difference between these two phases is small (~ 2 to 10 kJ/mol) [63]. The anatase structure is preferred over other polymorphs for solar cell applications because of its higher electron mobility, low dielectric

constant and lower density. The increased photoreactivity of anatase is due to the slightly higher Fermi level, lower capacity to absorb oxygen and higher degree of hydroxylation [64]. Brookite TiO_2 belongs to the orthorhombic crystal system. Its unit cell is composed of 8 formula units of TiO_2 and is formed by edge-sharing TiO_6 octahedra. It is more complicated, has a larger cell volume and is also the least dense of the 3 forms and is not often used for experimental investigations [65].

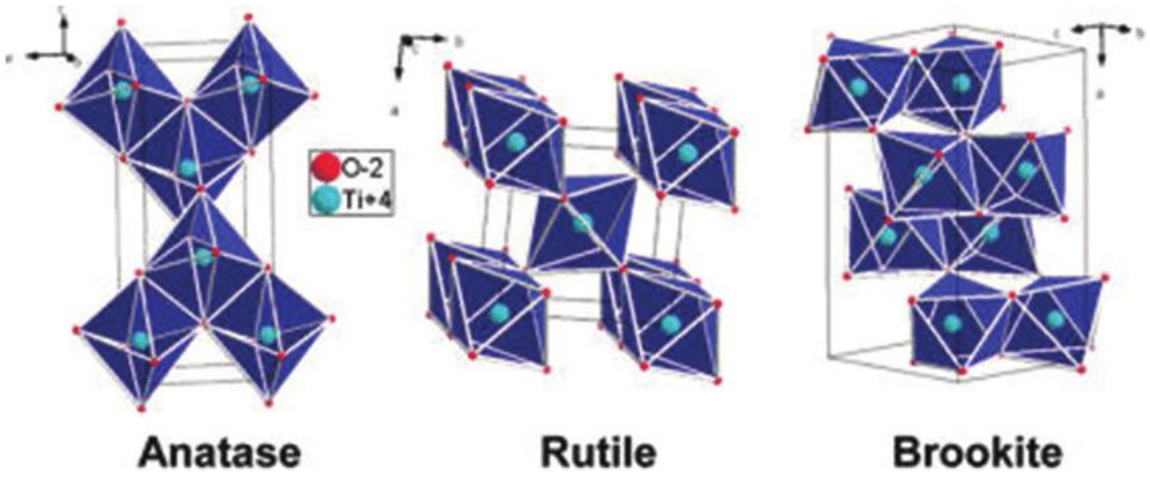

Figure 1.4: 3D arrangement of the TiO_2 anatase, rutile, and brookite forms [66].

1.2.2.2. Chemical properties

TiO_2 is considered very close to an ideal semiconductor photocatalyst due to its high oxidation efficiency, nontoxicity, high photostability, chemical inertness, and environmentally friendly nature [54,67]. TiO_2 semiconductor is an excellent photocatalyst, under UV irradiation it can mineralize a large range of refractory organic pollutants such as herbicides, dyes, pesticides, and phenolic compounds [15]. TiO_2 could be activated under UV irradiation having a wavelength lower than 387 nm due to its large band gap (3.0−3.2 eV) [15]. It absorbs only a small fraction of solar light (less than 5% of solar energy is emitted as UV irradiation) [15]. This major drawback limits the TiO_2 large scale applications. Owing to the successful results at the laboratory scale, TiO_2 material merits further research, in particular concerning the environmental applications at large scale.

1.2.2.2.1. Mechanism of TiO_2 photocatalysis

The semiconductor TiO_2 has been widely utilized as photocatalyst for inducing a series of reductive and oxidative reactions on its surface. When photon energy (hν) greater than or equal to the band gap energy of TiO_2 is illuminated onto its surface (usually 3.2 eV for anatase or 3.0 eV for rutile), the electrons are photoexcited to the empty conduction band in femtoseconds [58]. The light wavelength for such photon energy usually corresponds to $\lambda < 400$ nm [15]. The photonic excitation leaves behind an empty unfilled valence band, thus creating an electron-hole pair. The series of chain oxidative reductive reactions that occur at the photon activated surface was widely postulated as follows [58]:

Excitation of the catalyst:	$TiO_2 + h\nu \rightarrow e^- + h^+$	(5)
Charge – carrier trapping of e^-:	$e^-_{CB} \rightarrow e^-_{TR}$	(6)
Charge – carrier trapping of h^+:	$h^+_{VB} \rightarrow h^+_{TR}$	(7)
Electron-hole recombination:	$e^-_{TR} + h^+_{VB}(h^+_{TR}) \rightarrow e^-_{CB}$ + heat	(8)
Photoexcited e^- scavenging:	$(O_2)_{ads} + e^- \rightarrow O_2^{\bullet -}$	(9)
Oxidation of hydroxyls:	$OH^- + h^+ \rightarrow OH\bullet$	(10)
Photodegradation by OH•:	$R\text{-}H + OH\bullet \rightarrow R'\bullet + H_2O$	(11)
Direct photoholes:	$R + h^+ \rightarrow R^+\bullet$	(12)
Protonation of superoxides:	$O_2^{\bullet -} + OH\bullet \rightarrow HOO\bullet$	(13)
Co- scavenging of e^-:	$HOO\bullet + e^- \rightarrow HO_2^-$	(14)
Formation of H_2O_2:	$HOO^- + H^+ \rightarrow H_2O_2$	(15)

1.2.2.2.2. Structural design of TiO_2 photocatalysts

The construction of TiO_2 nano- or micro-structures with interesting morphologies and properties has recently attracted considerable attention and many TiO_2 nanostructural materials, such as nanospheres, nanorods, fibers, tubes, sheets, and interconnected architectures (**Figure 1.5)**, have been fabricated [68]. Structural dimensionality is a factor which can affect the photocatalytic performance and also has a significant impact on the properties of TiO_2 materials.

For example, **TiO_2 spheres** (**Figure 1.6-a)** with zero dimensionality are the most widely studied and used in TiO_2 related materials [68]. They are typically prepared from titanium alkoxide such as titanium tetraisopropoxide or titanium tetrabutoxide, in the presence of a polymer. The particles obtained can be further treated by hydrothermal methods to produce porous or hierarchical structures. This TiO_2 sphere has a high specific surface area, high pore volume, and pore size, resulting in a higher rate of photocatalytic decomposition of organic pollutants. Furthermore, these structural features increase the light-harvesting capabilities of these materials because they enhance light use by allowing as much light as possible to access the interior [69].

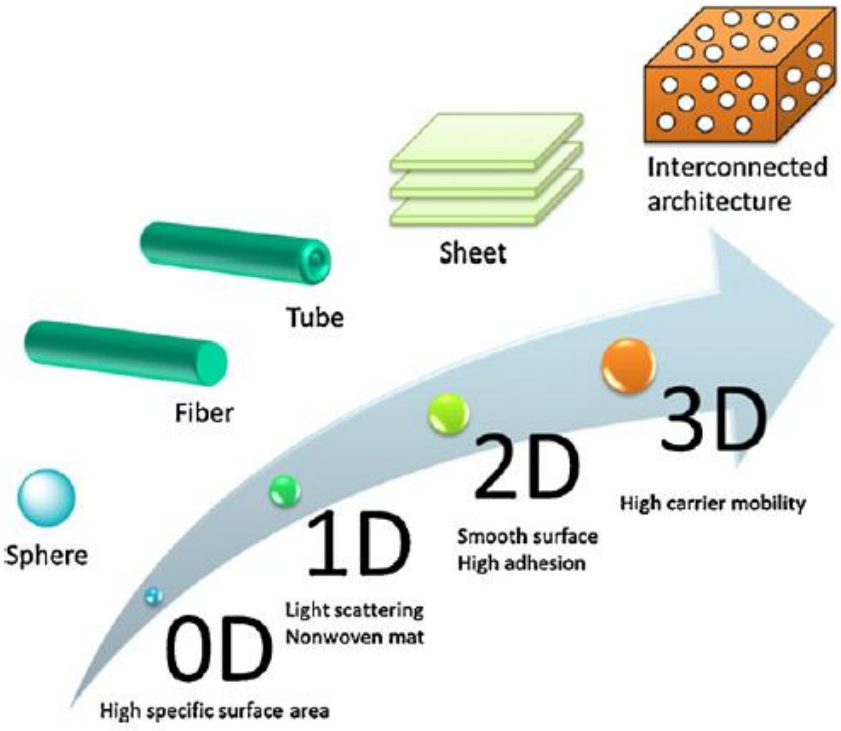

Figure 1.5: Different structures of TiO_2 material [68].

One-dimensional of TiO_2 such as **fibers (Figure 1.6-b)** or **tubes** (**Figure 1.6-c**) have the advantages of less recombination, high interfacial charge carrier transfer rate because of the short distance for charge carrier diffusion, and light-scattering properties [70]. TiO_2 fibers and tubes are typically prepared by electro-spinning of a mixture of

titanium alkoxide and a polymer, with a subsequent calcination step employed to remove the polymer and crystallize the TiO_2 [71]. The morphologies of the fibers can be controlled by varying a number of operation parameters such as changing the solvent concentration, molecular weight of the polymer, type of solvents, applied electric-field strength, and deposition distance.TiO_2 nanotubes were readily fabricated by sol–gel methods, template-assisted methods, hydro/solvothermal approaches, and electrochemical anodic oxidation [72–74]. TiO_2 fibers and tubes have wide application in photocatalyst, gas sensing, and batteries.

Two-dimensional nanosheets (**Figure 1.6-d**) are nano sized flake-shaped material with a flat surface, the thickness of 1–10 nm and a lateral size ranging from the submicrometer level to several tens of micrometers [68]. TiO_2 nanosheets are typically prepared by alkaline hydrothermal process using TiO_2 powder as a precursor or from protonic titanate hydrates, followed by either calcination process or hydro/solvothermal process [75,76]. The shape results in low turbidity, excellent adhesion to substrates, and high smoothness. TiO_2 nanosheets show photocatalytic properties including the photocatalytic decomposition of organic molecules and super-hydrophilicity, under UV irradiation [68,75].

Three-dimensional of TiO_2 (**Figure 1.6-e**) hierarchical structures such as macro/mesoporous with pores have potentially large surface, which provides a significant advantage in the form of efficient diffusion pathways for guest species, such as organic pollutants, into the framework and ultimately supports efficient purification, separation, and storage [68]. Three-dimensional of TiO_2 prepared from titanium tetrabutoxide, followed by hydrothermal treatment, without the use of templates or additives [79]. The structural parameters of the material, such as pore size, pore volume, and specific surface area, and crystallinity, could be controlled by adjusting the hydrothermal reaction time. Therefore, choosing TiO_2 materials with the appropriate dimensionalities enables us to take full advantage of the unique properties offered by TiO_2 materials.

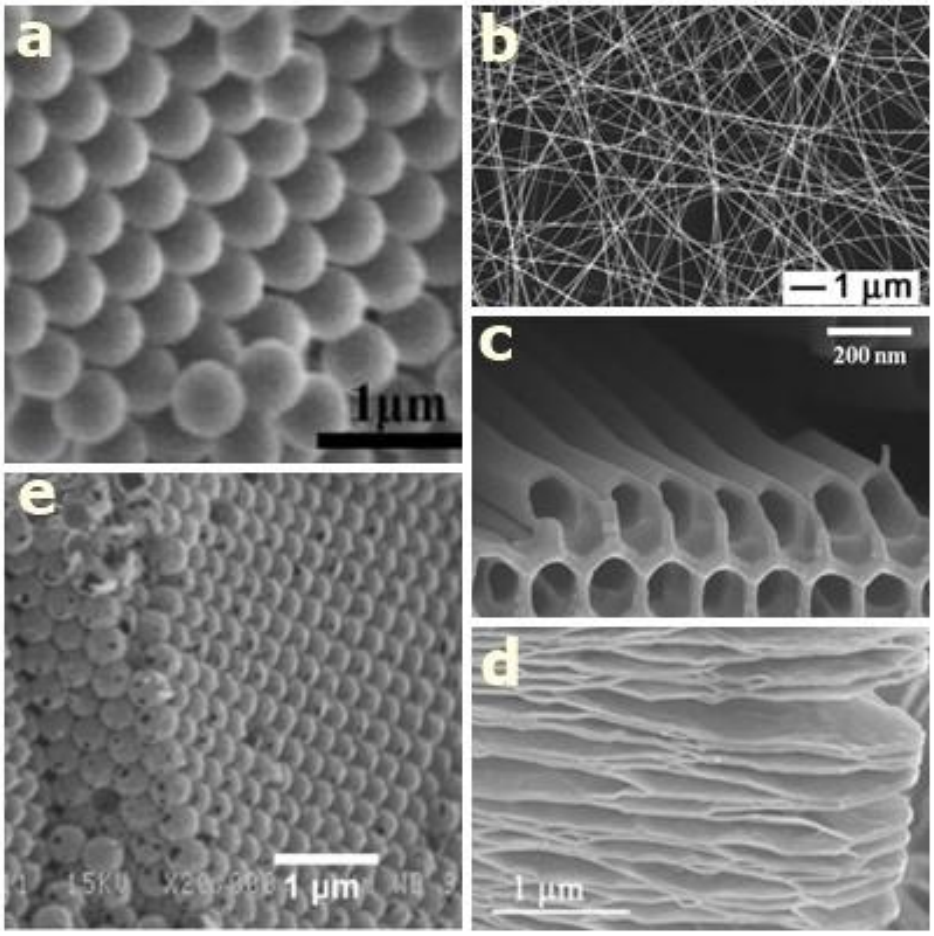

Figure 1.6: SEM image of different structures of TiO_2 material a) TiO_2 sphere; b) TiO_2 fibers [71] c) TiO_2 tubes [77]; d) TiO_2 sheets; e) TiO_2 three-dimensional [78].

1.2.3. Modifying TiO_2

As mentioned above, TiO_2 is closed to being an ideal photocatalyst due to its low price, photostability in solution, nontoxicity, and the fact that its electrons and holes are strongly oxidizing and redox selective. The most significant reason for the low conversion efficiency of TiO_2 under visible light is due to the width of the band gap, which is 3.2 eV and 3.0 eV for the anatase and rutile phase, respectively [60]. This relatively wide band gap means that both TiO_2 forms could be stimulated only under UV irradiation. Thus, the development of TiO_2 photocatalyst help to improve the properties of semiconductor, so it can absorb visible light region of the spectrum requires engineering the band gap to less

than 3.0 eV; suitable potentials of the conduction and/or valence band edges; and higher mobility of the charge carriers within in the valence and the conduction bands [15]. To overcome this large bandgap problem, several approaches including dye sensitization, doping, coupling and capping of TiO_2 have been studied extensively.

1.2.3.1. Dye sensitization

Dye-sensitized TiO_2 has received much attention in photocatalyst applications, such as dye-sensitized cells and generation of hydrogen from water. Dye sensitization can increase the efficiency of the excitation process and expand the wavelength range of excitation for the photocatalyst through excitation of the sensitizer followed by charge transfer to the semiconductor [80]. Charge carriers can be formed in semiconductor particles by exciting a dye attached to the surface of the photocatalyst. After that, the excited state can inject either a hole or an electron to the particle. Highly efficient charge injection is observed when a monolayer of a dye is dispersed on a photocatalyst with a high surface area [81]. Furthermore, the CB edge of lies slightly below the excited state energy level of many dyes, which is one condition required for efficient electron injection. Its high dielectric constant provides effective electrostatic shielding of the injected electron from the oxidized dye molecule, thus preventing its recombination before reduction of the dye by the redox electrolyte [82]. The high refractive index of TiO_2 results in efficient diffuse scattering of the light inside the porous photoelectrode, which significantly enhances light absorption [83].

1.2.3.2. Doping TiO_2

Doping is well known to be an effective way to alter the optical and electronic properties of semiconductors for different applications. Technically, doping is to decrease of the band gap or to introduction of intra-band gap states, which results in the absorption of more visible light. In photocatalysis, several approaches for TiO_2 modification such doping with metal (using transition metals: Cu, Ni, Fe, Au, Ag, Pt,...) [84–90], non-metal doped-TiO_2 (N, S, C, P,...) [91–95], are popular techniques that facilitate visible light activity of wide band gap semiconductors.

- *Factors influencing the performance of doped TiO_2*

Doping can result in a red-shift in the absorption spectrum of TiO_2 and consequently increase the photocatalytic activity of TiO_2 in the visible region. The extent to which the light absorption spectrum is red-shifted is dependent not only on the nature of the dopant but also on its concentration. A higher concentration of the dopant often leads to a greater redshift. However, the degree of red-shift is not always in line with photoactivity because in many cases doping ions can also act as trapping sites. Increasing the dopant concentration, therefore, may enhance the recombination of photogenerated electrons and holes, and consequently, lower the reaction rate [15].

- *Cation-doped TiO_2*

Titanium dioxide doped with cations such as rare earth metals, noble metals, poor metals, and transition metals have been widely investigated. The metallic ions-doped TiO_2 widen the light absorption range, increase the redox potential of the photogenerated radicals, and enhance the quantum efficiency by inhibiting the recombination of the electrons and holes photogenerated on the conduction and valence bands, respectively [15]. There is a large amount of research that demonstrates how metal ion doping of TiO_2 improves the visible light absorption properties of the material like $Pd/RuO_2/TiO_2$, Pd/TiO_2, CuO/TiO_2, $Cu–Fe/TiO_2$,…[43,84,86,88]. For example, Teh et al. [96] proved that iron (Fe) exhibits two or more oxidation states (Fe^{4+}, Fe^{3+}, and Fe^{2+}) (**Figure 1.7**) acts as a trap for the electron-hole pairs and consequently inhibits their recombination, that ensures an enhancement in the TiO_2 photocatalytic activity.

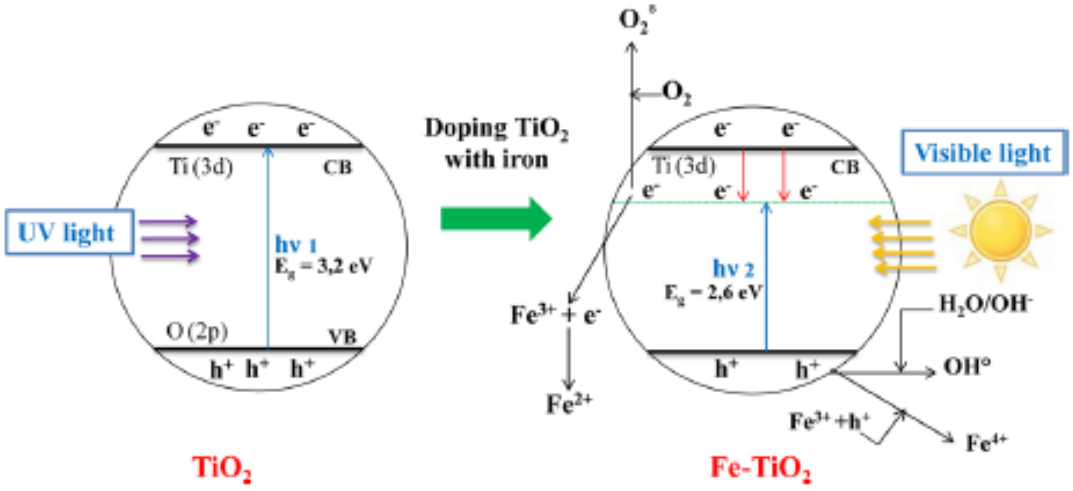

Figure 1.7: Schematic energy level of iron doping TiO_2 [15].

However, several authors have reported that metal doping TiO_2 have also considerable drawbacks. The photocatalytic activities of a cation-doped TiO_2 decrease even under UV irradiation. The metal-doped materials have been shown to suffer from thermal instability, and the metals centers act as electron traps, which encourage the recombination of the photogenerated electrons/holes pairs. With noble metals, the difference between the Fermi level of noble metals and that of titanic is ascribed to the electron−hole pair separation. If the metal centers become negatively charged, the hole will be attracted especially for highly loaded samples and the recombination is favored [15]. **Table 1.5** shows some examples of metal doping TiO_2 and their photocatalyst applications:

Table 1.5: Examples of metal doping TiO_2 and their applications.

Doped element	Method	Application	References
Ag	Sol-gel Method	Degradation of nitrophenol in aqueous phase	[97]
Fe	Hydrothermal Method	Wastewater treatment	[98]
Au	Photoreduction Process	Wastewater treatment	[99]
Pt	Photoreduction Process	Wastewater treatment	[100]

- *Anion- doped TiO_2*

Over the last several years, it has been demonstrated by many researchers that TiO_2 doped with nonmetal elements (carbon, sulfur, fluorine, nitrogen, etc.) [91–95] show positive effects in the visible region and higher photocatalytic activity. Nonmetal dopants have the ability to improve the morphology and the photocatalytic performance of TiO_2. The anionic metal doping of TiO_2 can lower its band gap and shift its optical response to the visible light region [15]. Conform to the research of Peng et al. [101] and Ao et al. [102] (**Figure 1.8**), N-doped TiO_2 had a narrower energy band gap (from Eg = 3.2 eV to Eg = 2,5 eV), which can be activated under visible light and also enhancing the photocatalytic activity.

In the doping of TiO_2 with an anion, the high surface area of the dopant sample is the main factor that increases the photocatalytic activity [96]. The higher surface area provides more reactive sites and promotes the adsorption of more target pollutants. Furthermore, many researchers showed that doping anion into TiO_2 could change the refraction index, hardness, electrical conductivity, elastic modulus, and the photocatalytic activity toward visible light absorption [96,103].

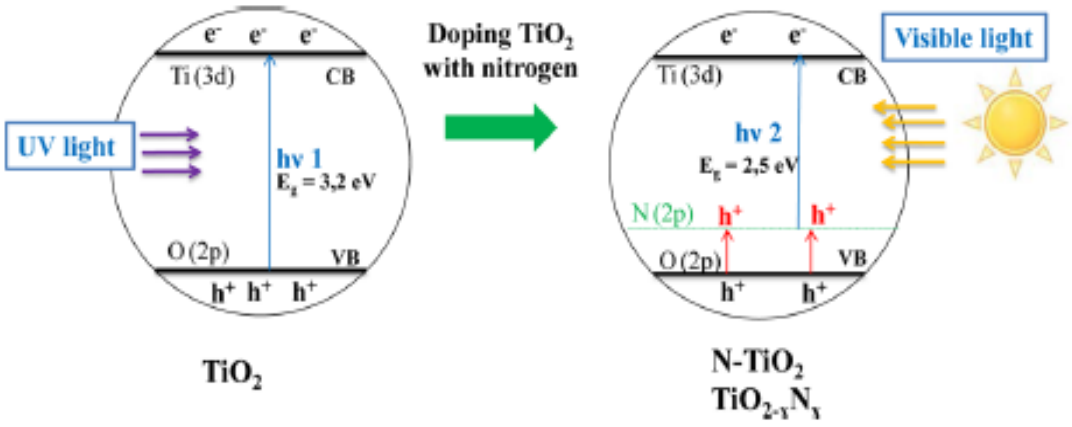

Figure 1.8: Schematic energy level of nitrogen doping TiO_2 [15].

The **Table 1.6** shows some examples of non-metal doping TiO_2 and their applications:

Table 1.6: Examples of non-metal doping TiO_2 and their applications.

Doped element	Method	Application	References
N	Titanium nitride (TiN) oxidation	Photooxidation of aromatic compounds (e.g. toluene)	[104]
	Treating TiO_2 powder in NH_3	Photooxidation of acetaldehyde in gas phase	[105]
S	Titanium disulfide (TiS_2) oxidation	Wastewater treatment	[106]
C	Sol-gel method	Photooxidation of phenol compounds in aqueous phase	[107]
P	Sol-gel method	Photooxidation of phenol compounds in aqueous phase	[108]

- *Co-catalyst*

Since TiO_2 NPs can only be excited by high energy UV irradiation with a wavelength shorter than 387 nm due to its relatively high energy band gap (3.2 eV), it is well known that coupling TiO_2 with others semiconductors as a co-catalyst can lead to an increase in photocatalytic efficiency by the enhancement of the charge carrier separation process and thus an increase in the lifetime of the charge carriers. In additional, the proper selection of coupled semiconductors can also activate the heterojunction system towards a visible light response [109,110]. When the large band gap of TiO_2 is coupled with another semiconductor, the energy gap between corresponding band levels drives the charge carriers from one particle to its neighbor to form a spatial separation between electrons and holes.

The coupling of semiconductors does not always enhance the charge separation, because the design of a coupled photoelectrode relies on the band structures of its components, which are determined by many other factors.

Depending on the band positions of two semiconductors forming heterojunction, three different types of heterojunction could be distinguished: I, II and III (**Figure 1.9**) [111]. Among 3 types, type II, which provides the optimum band positions for efficient charge carrier separation, is considered the most preferable for the coupled semiconductors based on TiO_2. Under UV–vis irradiation, both semiconductors are excited. Photoexcited electrons are transferred from CB(B) to CB(A) and this transfer can occur directly between semiconductors due to favorable energetics of the relative positions of CBs, or due to band bending at the interface inducing and internal electric field [111]. Whereas, holes are transferred simultaneously from VB(A) to VB(B) and as a result photogenerated electrons and holes are separated from each other, reducing the recombination probability and increasing the lifetimes of the charge carriers [15].

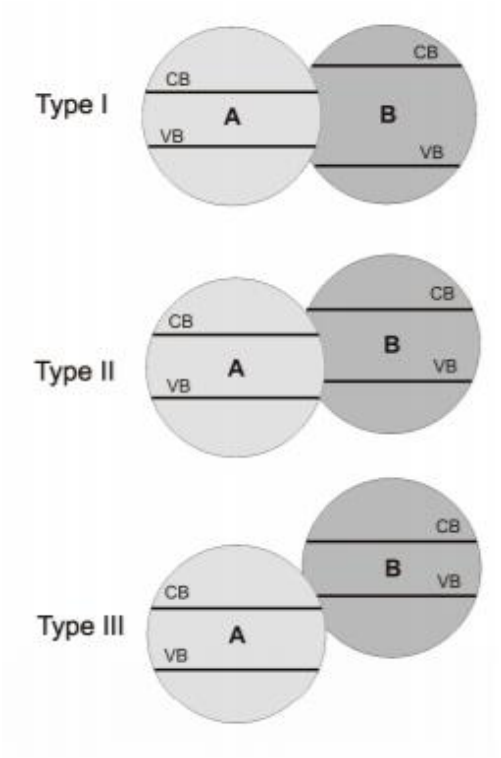

Figure 1.9: Types of heterojunction system of coupled semiconductors [111].

Several coupled colloidal structures of TiO_2, such as CuO/TiO_2 [88,112], Ag/TiO_2 [89,90], Pt/TiO_2 [113], Fe/TiO_2 [84], Co/TiO_2 [85], Ni/TiO_2 [86], etc, have been reported. Among them, the coupled structure of CuO and TiO_2 NPs has received the most attention.

1.2.4. Concept of heterojunction between copper oxides and titania

CuO are p-type semiconductors with band gap energies of 1.7 eV. The band positions of copper oxides in relation to TiO_2 are shown in **Figure 1.10** [111].

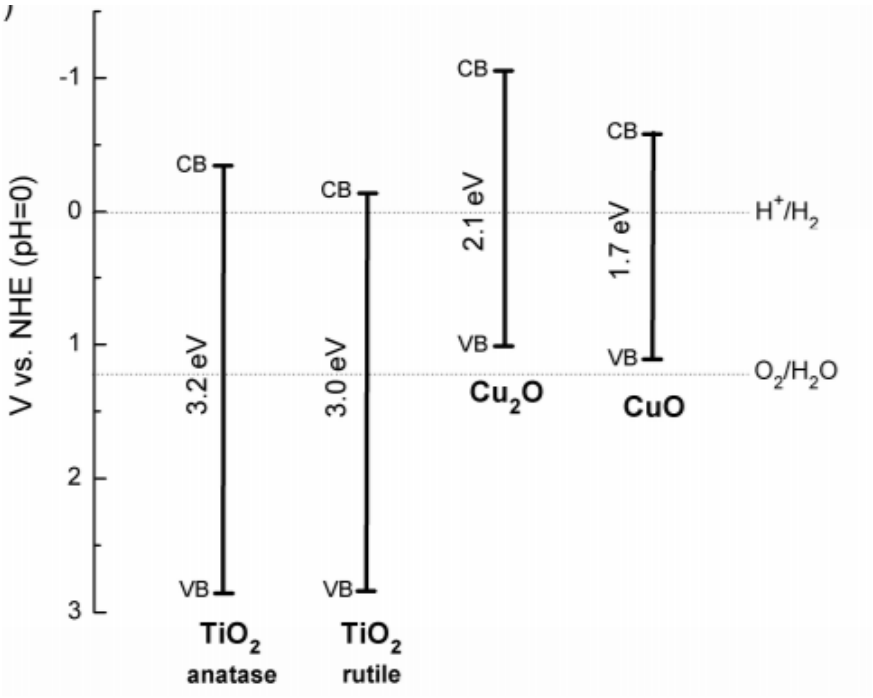

Figure 1.10: Band positions of copper oxides and TiO_2 [111].

The heterojunction between CuO and TiO_2 is a very promising way to improve the photocatalytic activity of titania under UV or/and visible light irradiation and to obtain more active and stable photocatalytic material than copper oxides or titania alone. For example, Chen et al. [114] reported that, depending on the copper loaded on TiO_2, CuO is found to be a sub-layer, for low Cu loaded, and in the form of nanosized particles and then bulk when more than 3.0% of Cu present on the semiconductor. These authors recorded a huge enhancement of reactivity passing from bare TiO_2 to CuO-TiO_2.

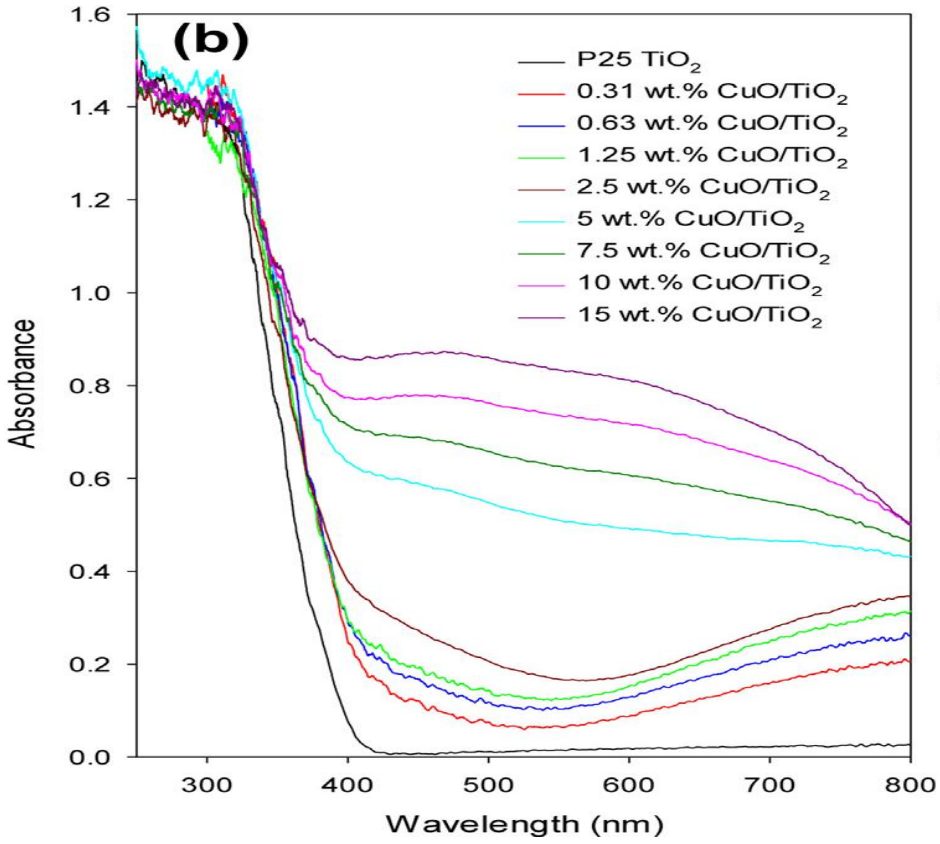

Figure 1.11: UV-visible absorbance spectra for the 0-15 wt.% CuO/P25 TiO_2 photocatalysts [114].

Figure 1.11 shows the UV-Vis absorbance spectra for the 0-15 wt.% CuO/TiO_2 photocatalyst. All samples displayed intense absorption below 400 nm due to the TiO_2 support. Deposition of CuO caused the samples to absorb strongly at visible wavelengths, though the visible absorption spectra differed considerably depending on the nominal CuO loading. At low CuO loadings (< 5 wt.% CuO), absorption features at 450 nm and above 800 nm were observed. At higher loadings (5 wt.% CuO and above), intense absorption across the entire visible spectrum was observed, consistent with CuO nanoparticle formation (bulk CuO absorbs very strongly between 300 and 900 nm). The intensity of the CuO related peaks increased with the nominal CuO loading in the range 5-15 wt.% CuO [114].

Other experiments have found that the incorporation of Cu^{2+} ions into a TiO_2 matrix can substitute for Ti^{4+} and/or segregate to the surface of TiO_2 crystallites in the form of CuO, Cu_2O or metallic Cu [115–118]. They showed that Cu loading can effectively narrow the band gap by creating impurity bands [116,117], and thus improve the absorption of visible light in photocatalytic reactions, therefore, improve significantly the photocatalytic activity.

Thus, in general, CuO/TiO_2 configuration can lead to increase in photocatalytic efficiency by: (a) an improvement of charge carriers' separation; (b) an increase in the lifetime of the charge carrier; and (c) an enhancement of the interfacial charge transfer efficiency to adsorbed substrates. However, the main limitation of their application results from not good photostability, which is very important issue for oxidative photocatalytic systems.

1.3. Applications of TiO_2 photocatalyst for environmental purification

Nowadays, the application of photocatalytic processes using TiO_2 as a semiconductor has been receiving much attention for water and wastewater treatment, to reduce the emerging organic pollutants such as hormones, phenolic compounds, pharmaceutical compounds, personal care products, and pesticides. Several review articles have been published on photocatalytic water treatment with generally positive results, indicating the potential of photocatalytic oxidation technologies for neutralizing very diverse categories of toxic compounds in water. For example, Asmussen et al. [119] reported wastewater remediation using bi-functional electrodes that performed both photocatalytic degradation and electrochemical oxidation. A thin film of TiO_2 was coated on one side of a Ti plate, while an electrocatalyst (thin film of Ta_2O_5-IrO_2) was coated on the other side. These bi-functional electrodes exhibited superb activity for the degradation of common persistent toxic pollutants (4-nitrophenol and 2-nitrophenol) in industrial and agricultural wastewater. Mahmoodi et al. [120] studied the photocatalytic degradation of a textile dye (Acid Blue 25) in a photocatalytic reactor containing immobilized TiO_2 nanoparticles and showed that immobilized TiO_2 nanophotocatalysis was capable of

degradation of Acid Blue 25 in textile wastewater, reducing its toxicity. There are also various reports mentioned on the degradation of pesticides (herbicides, insecticides, and fungicides) using TiO_2 or modified TiO_2 in solution, as listed in **Table 1.7**.

Table 1.7: Degradation of pesticides using TiO_2 or modified TiO_2 in solution.

Pesticide	Category	Semiconductor Using	Reference
Malathion	organophosphorus insecticide	TiO_2/ZnO	[121]
Methamidophos	organophosphorus pesticides	TiO_2	[122]
Dichlofenthion	insecticide	TiO_2 powder	[123]
Bromophos ethyl Bromophos methyl	insecticide	TiO_2 powder	[123]
Parathion ethyl Parathion methyl	organophosphorus insecticide	TiO_2 powder	[123]
Atrazine	herbicide	TiO_2 powder	[123]
Cyanazine	herbicide	TiO_2 powder	[123]
Metobromuron	herbicide	TiO_2 P-25	[124]
Isoproturon	herbicide	TiO_2 P-25	[124]
Cinosulfuron	herbicide	TiO_2 P-25	[125]

Besides pesticides, organic compounds and AOP can cause changes in biological cycles, particularly in the photosynthesis process. Photocatalytic oxidation of organic

compounds and AOP is of considerable interest for environmental applications and in particular for the control and eventual elimination of hazardous wastes.

1.4. Literature review conclusion

In this section, we presented an introduction about the fundamentals of photocatalysis process and how it can be used to the decomposition of organic compounds. In addition, we talked about how the TiO_2 is used as the most famous semiconductor in photocatalyst and also the methods to increase the photocatalytic activity of a photocatalyst. Then, a brief introduction about co-catalysts, helped us to understand their important roles in photocatalysis application specially in decomposing organic compounds. Moreover, a discussion about various configurations of heterojunctions in semiconductors was presented.

TiO_2 as the most well-known semiconductor in photocatalyst thoroughly and the challenge to work effectively in visible light region was mentioned. We talked about various nanocomposites structures of TiO_2 with different effects on visible light active photocatalysts. In addition, the effects of applying heterojunctions in the improvement in decompose organic compounds were discussed together. The heterojunctions mostly increased hydrogen evolution due to the enhancement of charge separation process. In other words, one kind of photogenerated charge carriers (electrons) migrate from one semiconductor to another, and from there they reduced protons. However, the other photoexcited charge carriers (holes) stayed in the first photocatalyst. Therefore, charge recombination process declined significantly and so the decomposition organic compounds were improved.

After that, the titanate nanodisks load over SiO_2 nanospheres materials and its potentials such as a narrow band gap and challenges such as low specific surface area and high rate of charge recombination, to decompose organic compounds were discussed. Then, different approaches to improve its photocatalytic activity were reviewed. They are including creating heterojunctions with other semiconductors, using other metals (Cu, Ni, Pt) as co-catalysts or doping TiO_2 with a non-metal element (sulfur). Most of the methods

displayed an increase of specific surface area and the improvement in decompose organic compounds. Among different metals have been employed to narrow the band gap and enhance the light absorption of TiO_2, Cu is recognized as an efficient dopant because of its low cost, and its properties. The 3d orbitals of Cu dopants can form electron donor levels within the CB of TiO_2 leading the enhancement of visible light absorption. After H_2S treatment, Cu^{2+} could be converted into CuS, forms the CuS-CuO-TiO_2 dual co-catalyst which has a significant role in improving the charge separation and enhance the light absorption.

1.5. Objective of the research

TiO_2 semiconductor is an excellent photocatalyst that, under UV irradiation, can mineralize a large range of refractory organic pollutants such as herbicides, dyes, pesticides, and phenolic compounds. Its large band gap leads however to low quantum efficiencies in the visible light region. Therefore, the general objective of this research thesis is to synthesize and develop nanocomposite photocatalysts for increasing the photocatalyst efficiency of TiO_2 semiconductor. To achieve this aim, we work on different strategies to reduce the large band gap and to improve charge separation process. The specific objectives are the following:

(1) Synthesize and characterize TiO_2 nanoparticles (NPs). They will be obtained by modifying the structure of semiconductors or controlling the morphology of TiO_2 by synthesizing and loading titanate nanodisks over SiO_2 nanospheres.

(2) Investigate the effect of coupling with other metals (Cu, Ni, Pt) as co-catalysts and the application of different methods to provide some charge trapping centers such as doping TiO_2 with a non-metal element (sulfur).

(3) Evaluate the photocatalytic activity of the prepared new materials in the decomposition of an organic compound (aqueous methanol).

Chapter 2: Methodology

2.1. Chemicals

Titanium butoxide (TB, 97%), benzyl alcohol (BA, 98%), oleylamine (OM, 98%), benzyl ether (BE, 98%), tetraethylammonium (TEA) hydroxide, tetraethylorthosilicate (TEOS, 98%), polyethylenimine (PEI, 99%), ammonium hydroxide, methanol (99%) and toluene (98%) were purchased from Aldrich and Sigma Company.

2.2. Synthesis of titanate nanodisks

Titanate nanodisks (TNDs) were synthesized by the reaction of TB, BA and OM under non hydrolytic conditions *(***Figure 2.1)**. By controlling the operation condition like the reaction time, temperature, molar ratio of surfactants, uniform and size/shape-controlled TNDs can be produced [126].

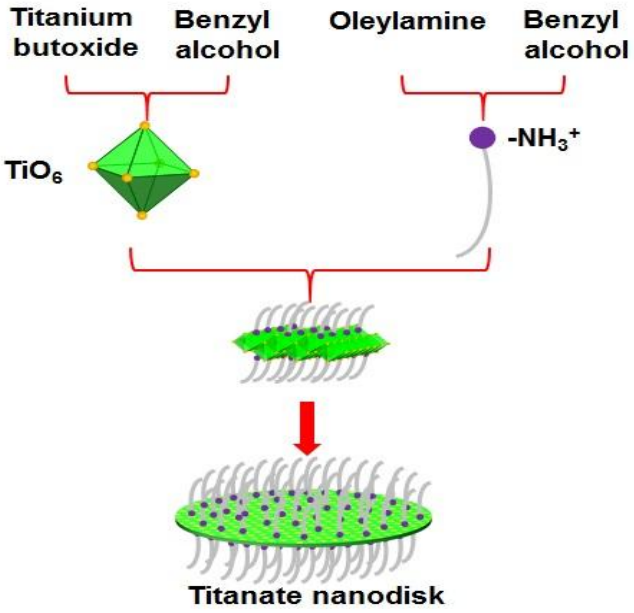

Figure 2.1: Illustration of the procedure for the design of titanate nanodisk [126].

To synthesize TNDs with the diameter of ~ 22 nm, 2 g of TB, 12 g of OM, 12 g of BA (OM:BA weight ratio of 1:1), and 30 g of BE were mixed in a flask. The mixture was kept under stirring for 30 minutes at room temperature before being transferred into a Teflon-lined stainless steel autoclave and heated to 180 $^{\circ}$C at the heating rate 5 $^{\circ}$C/min under nitrogen flow. After 20h, the reaction was stopped and cooled down to room temperature. The sample was washed several times using absolute ethanol to remove the unreacted reagents. The obtained nanodisks were then re-dispersed in toluene and re-precipitated by ethanol. This process was repeated a few times to remove the un-reacted reagents [126].

2.3. Synthesis of silica nanospheres

Silica nanospheres (SiO_2 NSs) were used as the based structure of the material. The size of SiO_2 NSs could be controlled easily by the Stöber synthesis [127]. To have the SiO_2 NSs with the diameter ~ 220 nm, TEOS (45 mL) was added to a mixture of ethanol (750 mL), H_2O (60 mL) and ammonia solution (40 mL, 28 wt.%). To obtain the diameter ~120 nm, 25 mL of TEOS was adding in the mixture solution of ethanol (750 mL), H_2O (60 mL) and ammonia (20 mL, 28wt %). After stirring for 4h at room temperature, the precipitated SiO_2 NSs were separated by centrifugation and washed 3 times with ethanol. The SiO_2 NSs were then re-dispersed in 100 mL of H_2O.

2.4. Synthesis of CuO/ TiO_2 nanospheres

The process of synthesis CuO/TiO_2 nanosphere combines three steps: coating TiO_2 nanodisks on SiO_2 nanosphere, coating CuO on TiO_2/SiO_2 nanosphere, and H_2S treatment of $Cu/TiO_2/SiO_2$.

2.4.1. Coating SiO_2 nanospheres with titanate nanodisks

SiO_2 NSs which were achieved from previous experiment were then coated with TNDs using a layer-by-layer deposition technique [128]. Typically, 5 g of SiO_2 NSs was dispersed in 200 mL of H_2O containing 0.2 g of polyethylenimine (PEI). The suspension

was stirred for 30 min to ensure the saturated adsorption of PEI on the surface of the SiO_2. Excess PEI was removed by centrifugation. The obtained PEI-coated SiO_2 was then redispersed in 200 mL of H_2O. After that, 10 mL solution of TNDs (containing 0.1 g TNDs) was gradually added to the SiO_2 NS suspension under stirring. Formation of flocculated aggregates in the mixture, which is caused by the electrostatic interaction of the negatively charged TNDs and positively charged PEI on SiO_2 surface, was observed after the addition of TND solution. The resulting material was then recovered by centrifugation and washing process. The above procedure was repeated for many cycles to obtain TND-PEI/SiO_2 NSs (**Figure 2.2**).

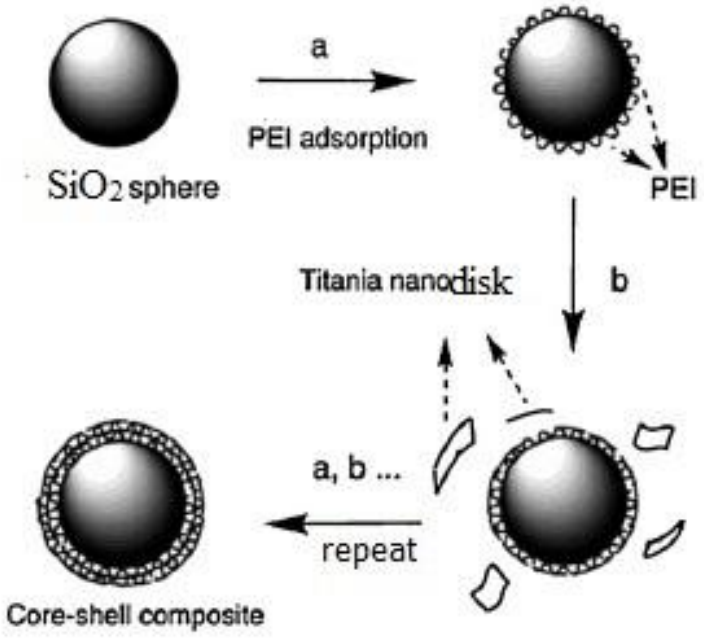

Figure 2.2: SiO_2 NSs were coated with TNDs using a layer-by-layer deposition technique [129].

2.4.2. Coating CuO on TiO_2/SiO_2 nanosphere

The obtained TND-PEI/SiO_2 nanospheres were re-dispersed in 200 mL of H_2O and 10 mL of Cu^{2+} solution (15 mM) was then added. The resulting mixture was stirred for 60

min to ensure the adsorption of Cu^{2+} on the TND-PEI/SiO_2 NSs. The obtained precipitate was dried at 60°C overnight and then calcined at 550 °C (ramp rate of 2 °C/min) for 4 hrs to obtain CuO/TiO_2/SiO_2. Ni^{2+}/TiO_2/SiO_2 and Pt^{2+}/TiO_2/SiO_2 were obtained by following a similar procedure (**Figure 2.3**).

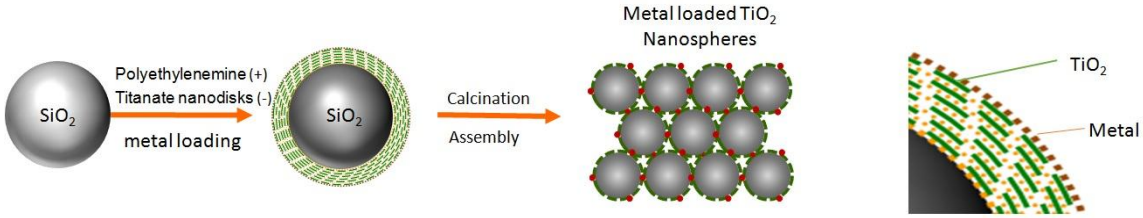

Figure 2.3: Schematic illustration of synthesis of metal loaded TiO_2 NSs.

2.4.3. H_2S treatment of CuO/TiO_2

After having CuO/TiO_2 with suitable concentration and morphology, this composite was heated to 450 °C at the heating rate 5 °C/min under H_2S flow of 4 L/h in 4 hrs for H_2S treatment.

2.5. Characterization

2.5.1. Electron microscopy

Electron microscopy is a technique which uses a beam of electrons for obtaining high resolution images of a selected area electron diffraction of the sample. These images could be the topology of the surface, the structure or the composition of this selected area electron diffraction. Electron microscopy could be categorized into two main types: transmission electron microscopy and scanning electron microscopy.

Transmission electron microscopy (TEM) can provide information about the orientation, atomic arrangements, and phase composition of selected area electron diffraction. TEM images of the samples were obtained on a JOEL JEM 1230 operated at 120 kV.

Scanning electron microscopy (SEM) produces images of topography, morphology, composition or crystallographic information of the selected area electron diffraction. SEM magnifications can go to more than 300,000 times (compare with the real size of the samples), on a nanometer (nm) to micrometer (μm) scale. SEM images were obtained on a JEOL 6360 instrument operated at 15 kV.

2.5.2. UV-visible absorption spectroscopy

UV-visible (UV-vis) absorption spectroscopy is useful for quantitative measurements, characterization of absorption, transmission, and reflectivity of a variety of materials.

UV-vis uses light in the visible and adjacent near ultraviolet (UV) ranges. The UV-vis light is passed through a solution (or thin film), and a detector collects the transmitted light. The difference between a transmitted light from a reference and a target sample permits to measure the photoabsorption properties and concentration. Therefore, this technique is exerted to analyze the organic dyes, metal or semiconductor nanoparticles highly dispersed in a solution. The UV-vis spectra were recorded on a Cary 300 Bio UV-visible spectrophotometer.

2.5.3. Specific surface area analysis

The specific surface area was determined from nitrogen adsorption using the Brunauer−Emmett−Teller (BET) method to calculate the specific surface area. The generalized BET equation for gas adsorption can then be described as follows [130]:

$$\nu = \frac{\nu_m c p}{(p_0 - p)[\,1+(c-1)\left(\frac{p}{p_0}\right)]} \qquad (16)$$

where ν is the adsorbed volume of gas (m^3)

ν_m is the adsorbed monolayer volume (m^3)

p is the equilibrium gas pressure (Pa)

p_0 is the saturation gas pressure (Pa)

c is the BET constant

This equation can then be rearranged as a linear function of p/p_0 as follows:

$$\frac{1}{\nu\left[\left(\frac{p}{p_0}\right)-1\right]} = \frac{c-1}{\nu_m c}\left(\frac{p}{p_0}\right) + \frac{1}{\nu_m c} \qquad (17)$$

The specific surface area (m^2/kg) can be found by the equation:

$$S = \frac{\nu_m \, NA}{22400 \times m} \qquad (18)$$

where N is Avogadro's number (6.022×10^{23} mol^{-1})

A is the cross-sectional surface area of a single adsorbed gas molecule (m^2)

m is the mass of nanomaterials used in the measurement (kg)

$22{,}4 \times 10^{-3}$ is the standard temperature and pressure (STP) volume of one mole of gas ($m^3 \cdot mol^{-1}$)

2.5.4. Photodecomposition of methanol and gas chromatography analysis

Photocatalytic reaction of the composite photocatalysts were carried out in a top-down-type photoreactor connected to a closed-gas circulation system. An amount of photocatalyst (0.1 g) was dispersed in a 5000 ppm solution of methanol in water. The reaction cell was then filled with fresh synthetic air (Prax air) and stirred for 1h to reach the steady-state regime. Then, the cell was illuminated with a solar simulator (150 W Xe lamp AM 1.5 G, 100 $mW \cdot cm^{-2}$) for 3 hrs.

Gas chromatography (GC) analysis is a useful analytical separation technique to identify and determine different types of compounds. In the present work, the amount of

methanol produced in the reaction was analyzed using a GC (Agilent 7820A) equipped with a TCD and HP-PLOT U column, with helium as the carrier gas. The headspace volume is 20 mL, and the injected volume is 500 μL. **Figure 2.4** shows the testing systems for photodecomposition of methanol.

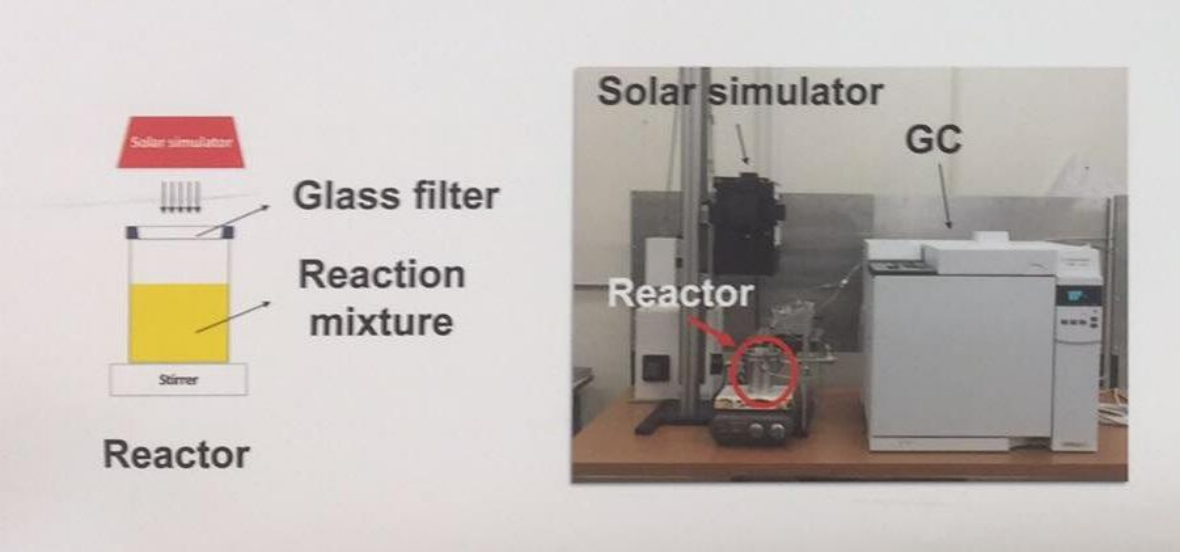

Figure 2.4: Testing systems for photodecomposition of methanol.

Chapter 3: Results and discussion

3.1. Results of titanate nanodisks synthesize

Titanate nanodisks (TNDs) were synthesized by the reaction of TB, BA, and OM under non hydrolytic conditions (**Figure 2.1**). The morphologies of TiO_2 nanoparticles were closely controlled by the existence of surfactants, especially the amount of BA used plays an important role in controlling the diameter of the nanodisks [126,132,133]. According to the literature, it has been also reported that BA can be used as a medium for the formation of a variety of metal oxides. The non hydrolytic reaction between BA and TB yields TiO_6 octahedra, results in the formation of primary TNDs building units; while protonated OM at elevated temperature by BA, balances the negative charge of the TNDs. In the absence of OM, a large amount of anatase TiO_2 NPs was formed, while in the absence of BA, no NPs were formed. Hence, the amount of BA used may directly affect the crystallization process and consequently the size of resulting of TNDs.

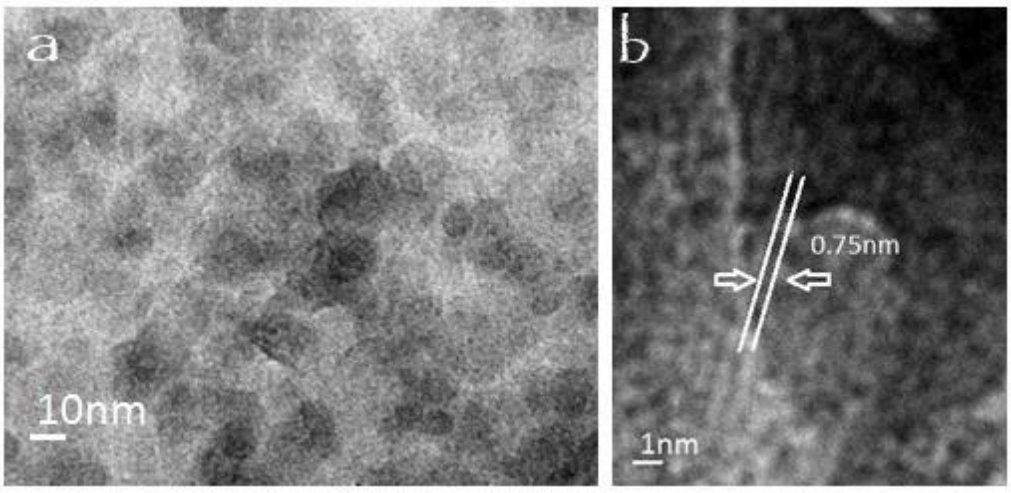

Figure 3.1: a) TEM image of TNDs; b) HRTEM image of TNDs parallel.

Figure 3.1-a shows representative TEM images of obtained TNDs with uniform size and a mean diameter of 20 nm while using the molar ratio between TB and OM is 1:6. The result was similar to results achieved in previous articles [126]. To estimate the

thickness of TNDs, they were dispersed in ethanol and analyzed by TEM. **Figure 3.1-b** shows the parallel layers structure of TNDs which are ultra thin (around 0.75 nm), and self-assembled in ethanol solution.

3.2. Controlling the size of SiO_2

During the synthesis, Tetraethyl orthosilicate (TEOS) was used as the precursor. Ammonia and distilled water were used as the catalyst and the hydrolyzing agent, respectively. Then ethanol was used to remove the initial materials that provide no reaction from the surface of the formed particles [134]. When TEOS was added into ethanol solution with the presence of ammonia as a catalyst, TEOS is hydrolyzed to produce the intermediate $[Si(OC_2H_5)_4\text{-}X\ (OH)_X]$ ions. Silanol groups are produced via the former process shown by reaction (19), which acts as a substrate for reaction (20), leading to a three-dimensional cross-linked network structure as a result of the latter process due to the formation of siloxan bridges (Si-O-Si).

$$Si(OC_2H_5)_4 + 4H_2O \xrightarrow{Suspension\ in\ ethanol} Si(OH)_4 + 4C_2H_5OH \qquad pH\ 11\text{-}12\ (NH_3) \qquad (19)$$

$$Si(OH)_4 \xrightarrow{Suspension\ in\ ethanol} \text{nano-}SiO_2 + 2H_2O \qquad pH\ 11\text{-}12\ (NH_3) \qquad (20)$$

Figure 3.2 illustrates the SEM characterization of SiO_2 nanospheres. SiO_2 with diameters of 120 nm, and 220 nm were synthesized as result from using 25 mL and 45 mL TEOS as precursors, respectively. The concentration of SiO_2 in the sol was determined from the weight of the collected and heat-treated (at 1000°C) particles versus the total weight of the prepared sol. The size of SiO_2 increased when we increased the concentration of TEOS, which is in good agreement with research from Dabbaghian et al. [80]. As the TEOS concentration is increased; the rate of hydrolysis become faster, result in more intermediate $[Si(OC_2H_5)_{4\text{-}X}\ (OH)_X]$ ions is generated. However, when it reaches the super saturation region, the consumption rate of intermediate through condensation reaction is

also relatively fast, which probably shortens the nucleation period. Thus, they have more chance to collide and form gel network, resulting in large particles.

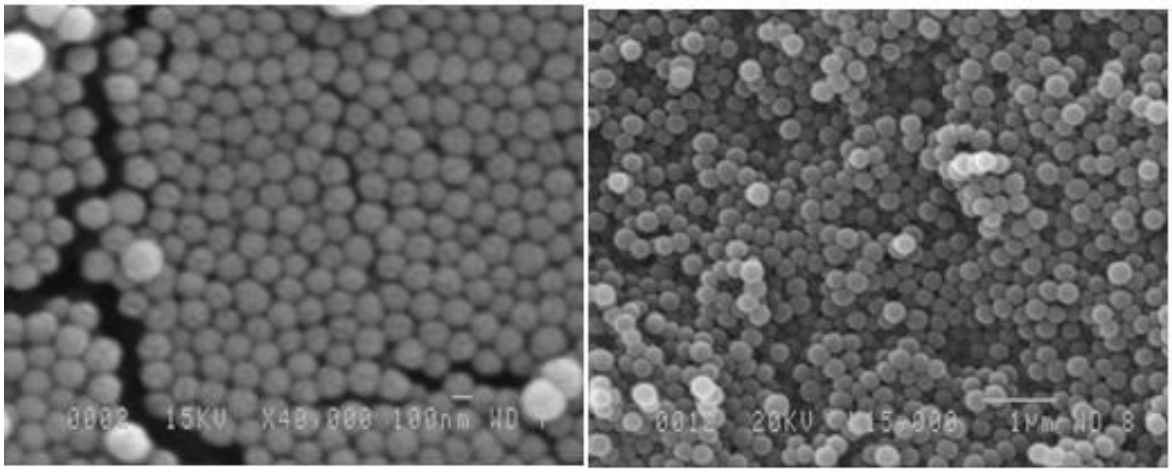

Figure 3.2: SEM image of different size of the material: d ~120 nm (left); d ~220 nm (right).

3.3. Nanosphere size and loading concentration of TiO_2 in photocatalytic property of TiO_2-SiO_2 nanosphere

Figure 3.3 shows the surface morphology of TNDs modified 120-nm-diameter silica particles after 10 times layer-by-layer coating technique. The particle diameter (d) size was increased 10 nm (from d ~ 120 nm to d ~ 130 nm) and the specific surface area of $CuO/TiO_2/SiO_2$ nanosphere increased from 20 m^2/g to 109.36 m^2/g.

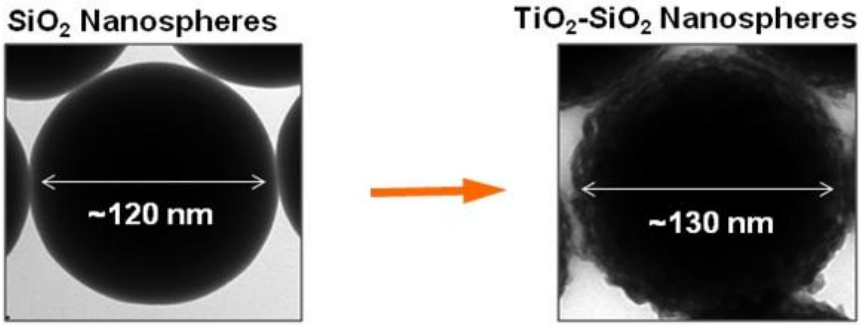

Figure 3.3: The size changing after layer-by-layer deposition technique.

The blank TiO_2 catalyst (Cu loading = 0 wt. %) appeared white, with the increasing of Cu deposition, the color of the material turn. It was observed that the adsorption of Cu^{2+} on the TND-PEI/SiO_2 NSs has the color light green, but after calcinated their color change to darker green indicating that Cu^{2+} oxidized into CuO, becomes CuO/TiO_2/SiO_2 nanospheres (**Figure 3.4**).

Figure 3.4: CuO/TiO_2/SiO_2 powder after calcination.

Follow the experiments of Chen et al. [114], depending on the copper load on TiO_2, the light absoprtion of the material could be effected. If the amount of Cu^{2+} loading to high (from 5 wt.% to above), the CuO residue can be formed after the reaction. This CuO excess can serve as a separate semiconductor in photocatalysts [135], but does not help in increasing photocatalytic activity of TiO_2. Therefore, the first experiment was conducted with a concentration of Cu^{2+} from 2 - 7 wt.% in order to find the most suitable concentration of CuO in the following modifying methods.

In addition, we examine how the morphological factors affect to the photocatalytic effect of TiO_2 by comparing materials with two different nanosphere particle sizes d ~ 120 nm and d ~ 220 nm.

The shift of optical absorption (**Figure 3.5**) is attributed to the presence of CuO. Compared with TiO_2 blank sample, the absorption edges of all Cu incorporated TiO_2

samples had a slight red-shift, which was most likely resulted from the incorporation of CuO in the TiO_2 matrix. The remarkable increase in the absorption at around 400 nm could be assigned to the presence of Cu species [136]. At the same time, it is found that the more obvious red-shift of absorption edges was, the more enhanced absorption in the visible light region was [116]. Moreover, the higher absorption intensity corresponds to a faster formation rate of electron–hole pairs on the photocatalyst surface. Thus, CuO/TiO_2 photocatalyst should exhibit higher photocatalytic activity. The experimental tests also revealed that at low Cu^{2+} solution loadings (<5 wt.% CuO), the material had stronger absorption UV-wavelengths compared to the higher loading. The concentration of Cu^{2+} providing the maximized photocatalytic efficiency is 2 - 7 wt.% relative to TiO_2. The results obtained were in good agreement with the 3 wt.% CuO/TiO_2 representing the best performing sample, approximately 1.4 times better of that of pure TiO_2 sample. Furthermore, the size also affect to the photocatalytic efficiency when the material has a smaller diameter, it does not only have higher specific surface area, but also better absorption capacity.

Therefore, after testing the effect of size and concentration, the particle size with diameter of 120 nm and the concentration of cation solution about 3% relative to TiO_2 was chosen.

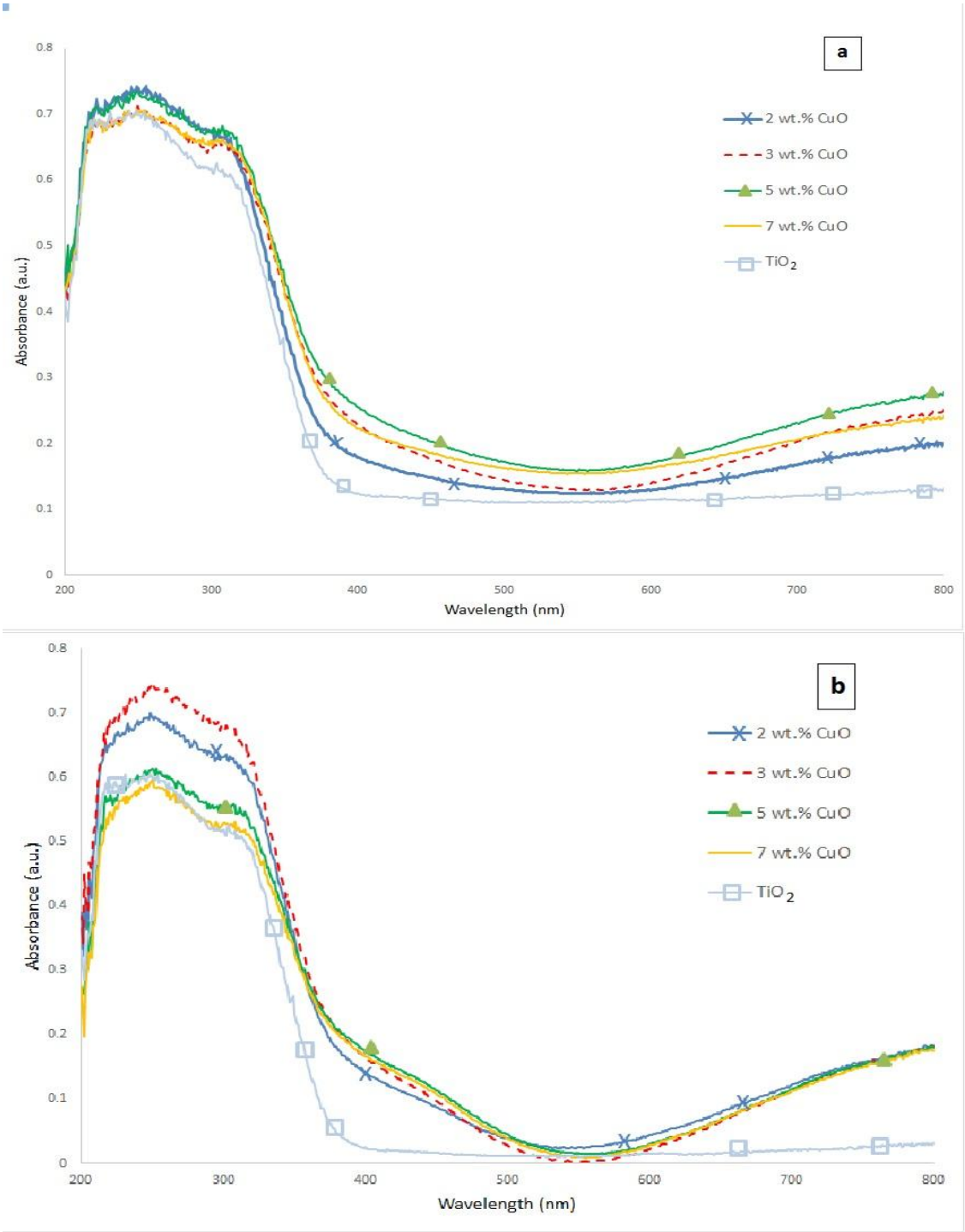

Figure 3.5: UV-Vis absorption spectra of different particle size and concentration of Cu^{2+} loading over TiO_2/ SiO_2 (a: d ~ 120nm; b: d ~ 220nm).

The photocatalytic activity of $CuO/TiO_2/SiO_2$ nanospheres was investigated in the photocatalytic decomposition of methanol under visible light illumination ($\lambda \geq 420$ nm). **Table 3.1** shows the amount of decomposition of methanol during 3 hrs of visible light illumination using TiO_2/SiO_2 nanospheres blank sample without loading CuO and $CuO/TiO_2/SiO_2$ nanospheres with diameter around 120 nm at different concentration of Cu^{2+} loading (at same condition and the amount of photocatalyst material is 0.1 g).

Some authors [137] reported an overall oxidation reaction of the decomposition of methanol based on the use of TiO_2:

$$TiO_2 \xrightarrow{UV\ irradiation} TiO_2\,(h^+ + e^-) \quad (21)$$

$$TiO_2\,(h^+) + CH_3OH + H_2O \rightarrow 6\,H^+ + CO_2 \quad (22)$$

On other hand, Choi et al. [138] tried to go further into the details of the process, considering the intervention of OH radicals formed from H_2O/OH^- reaction with positive holes:

$$CH_3OH \xrightarrow{h\nu} :CH_2 + H_2O \xrightarrow{.OH} \bullet CH_2OH \xrightarrow{.OH} CH_2(OH)_2 \quad (23)$$

Table 3.1: Decomposition of methanol using CuO/TiO_2 NSs with different concentrations of Cu^{2+} loading.

Sample	% decomposition
Without CuO	34.4
CuO/TiO_2 2 wt.%	32.4
CuO/TiO_2 3 wt.%	50.8
CuO/TiO_2 5 wt.%	42.6
CuO/TiO_2 7 wt.%	42.8

It can be seen that CuO/TiO_2 nanospheres can decompose methanol under visible light illumination in a higher extent compared to TiO_2 material. While at 3 wt.% CuO loading gives the highest UV absorption and gives the highest yield of decomposition methanol because photo-dissolution of Cu^{2+} particles by accepting photogenerated electrons and leaching to the reaction solution may occur. Therefore, the loading of CuO over TiO_2 was found to have higher photocatalytic activity than the TiO_2 blank sample, for working in UV-Vis spectra some reactions.

3.4. Effect of different metals loading over TiO_2

For material with the particle size of 120nm and the concentration of cation solution about 3% relative to TiO_2 as chosen above, the effect of two other metals (Ni, Pt) loading was investigate and compare with CuO loading. The method was used is photodecomposition the solution of cation Ni^{2+} (3 wt.%) and Pt^{2+} (3 wt.%). The BET tests showed that CuO/TiO_2 have a larger specific surface area 109.36 m^2/g compared to 3 wt.% Ni/TiO_2 (98.24 m^2/g) and of 3wt.% Pt/TiO_2 (67.15 m^2/g).

Figure 3.6 displays the UV-Vis absorption spectra of Cu, Ni and Pt loading over TiO_2. The absorption edges of all materials incorporated TiO_2 samples had a slight red-shift, which was most likely resulted from the incorporation of all Cu, Ni or Pt in the TiO_2 matrix. The increase in the absorption at around 250 - 300 nm could be assigned to the presence of Ni and Pt species [139,140]. As mentioned in the section **3.3**, the more obvious red-shift of absorption edges was, the more enhanced absorption in the visible light region was [116]. The light absorption capacity of Cu over TiO_2 is quite good compared to the other two materials, in both UV and visible light.

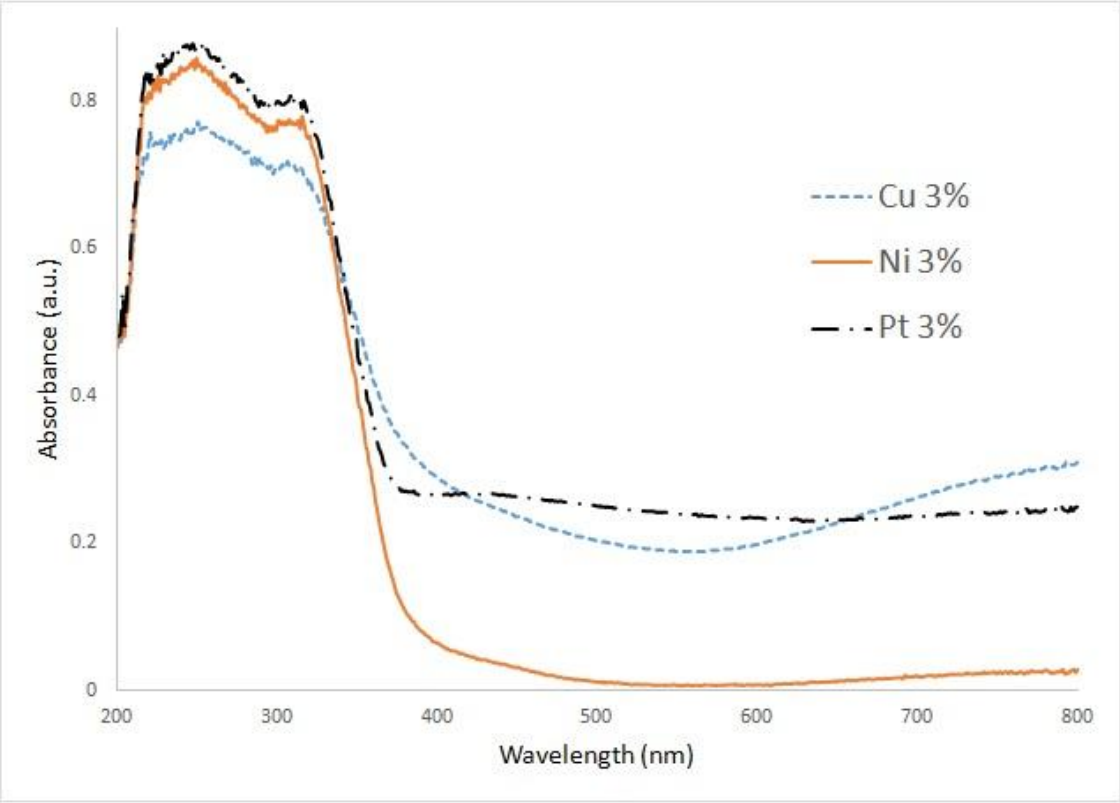

Figure 3.6: UV-Vis absorption spectra of different metals loading over TiO_2.

The three TiO_2 samples loaded with Cu, Ni or Pt were tested for the photodegradation of methanol in aqueous solution under solar light irradiation. With the same condition and same amount of photocatalyst material, the average of methanol degradation is 50.8%, 48.9% and 31.2% for Cu, Pt and Ni loaded, respectively (**Table 3.2**).

Table 3.2: Decomposition of methanol using Cu, Pt and Ni loaded over TiO_2.

Sample	% decomposition
3wt.% Cu loaded TiO_2	50.8
3wt.% Pt loaded TiO_2	48.9
3wt.% Ni loaded TiO_2	31.2

It was found that 3 wt.% Cu loaded TiO_2 and 3 wt.% Pt loaded TiO_2 have similar rate of methanol decomposition (50.8% and 48.9%, respectively). The most commonly ascribed effect of Pt and Cu is their ability to promote charge carrier separation with electrons being accumulating on the metal and holes remaining on TiO_2 [141,142]. The sources of enhancement in photocatalytic reactions on TiO_2 due to supported Pt and Cu include: a greater electron scavenging capability for O_2 [143], enhanced surface chemistry that redirects mechanisms and assists in removing strongly bound intermediates that might impede activity [144,145], de-aggregation TiO_2 particles in suspensions [146], promotion of OH• formation and promotion of proton reduction to adsorbed H atoms [147]. It can be concluded that the use of CuO/TiO_2 in photocatalysts is more effective than that of the two metals being compared. The results not only prove that the light absorption capacity of CuO/TiO_2 is good in wide band, but also the decomposition of methanol is extremely effective.

3.5. Effect of H_2S treatment

The incorporation of non-metals, including nitrogen, carbon, sulfur, fluorine, or iodine [91–95] was found to be a efficiency way to lower the band gap of TiO_2, thus obtaining a photocatalyst with high activity. As example, sulfur-doped TiO_2 has attracted much attention due to the fact that S can reduce the band gap, demonstrate a strong absorption in the visible light [95]. The 3 wt.% CuO/TiO_2 particle diameter 120 nm was heated to 450 $^{\circ}C$ at the heating rate 5 $^{\circ}C$/min under H_2S flow. While the green color of CuO/TiO_2 changes to very dark color (**Figure 3.7**). The color could be the result of new material created after S doped TiO_2.

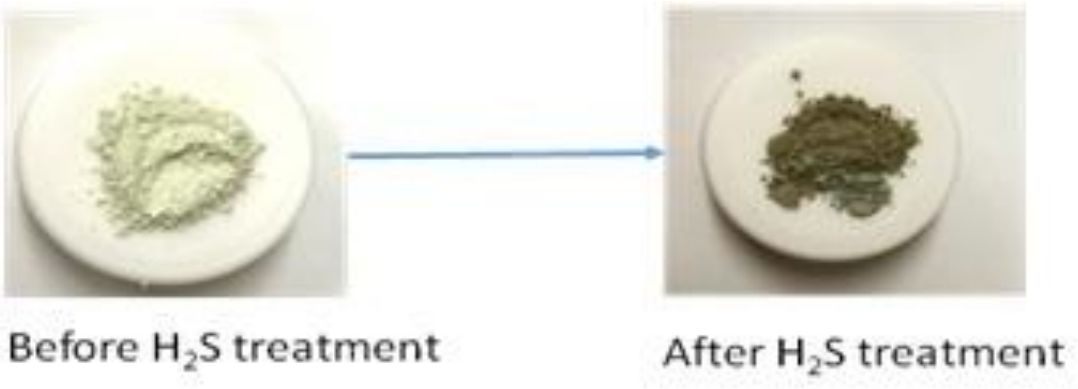

Figure 3.7: Color change of 3 wt.% CuO/TiO_2 after H_2S treatment.

There is a slight decrease of the specific surface area (82,12 m^2/g) comparing to the specific surface area of 3 wt.% CuO/TiO_2, observed after the H_2S treatment, which can be explained by the moderate sintering effect due to annealing treatment conditions occurring at 450 $^{\circ}C$ under an H_2S atmosphere. The UV-Vis spectrum of S-doped 3 wt.% CuO/TiO_2 (line curve) is compared with 3 wt.% CuO/TiO_2 (dash curve) in **Figure 3.8**. A wide shift of the absorption edge for the S-doped 3 wt.% CuO/TiO_2 sample towards higher wavelengths (lower energies) is clearly detectable, together with an additional wide absorption centered at around 370 - 390 nm.

This shift is associated with a change of TiO_2 electronic structure, during the treatment with H_2S, which causes the $S \rightarrow O$ exchange at the surface of TiO_2 [148,149]. Taking into consideration this aspect, it is well known that the formation of doping states involves additional electronic levels that can be formed between the VB and CB, thus reducing the electron transition energy [150]. Furthermore, the presence of the donor dopants (hydrogen) may enhance the acceptor (sulfur) incorporation in TiO_2 because of their strong electrostatic attractive interaction, leading to a decrease of recombination between electron-hole [151].

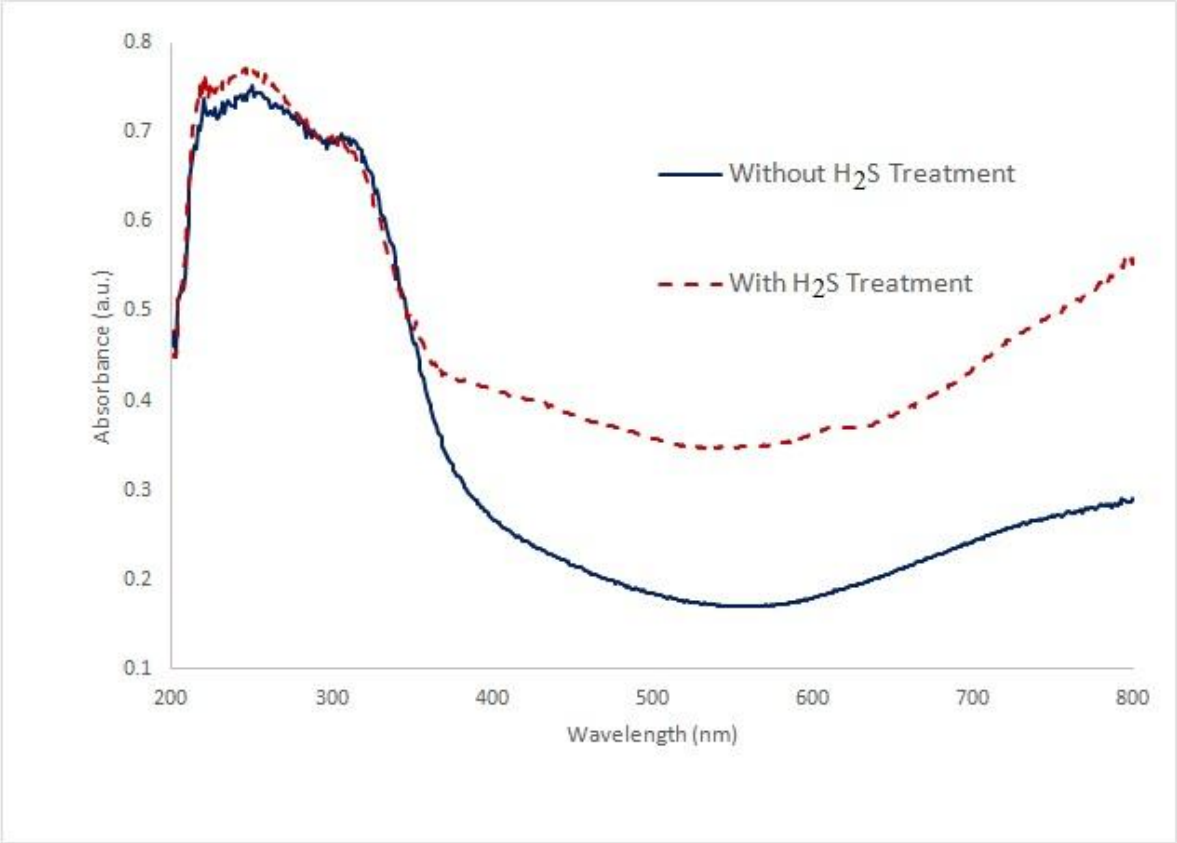

Figure 3.8: UV-Vis absorption spectra of CuO/TiO_2 3wt.% with and without H_2S treatment.

Furthermore, in decomposition of methanol in particular or organic matters in general, with H_2S treatment, at low temperature (lower than 300 ºC), the Ti-SH was created, which is very strong. However, at temperatures higher than 300 ºC, S-H becomes weaker and finally breaks. Therefore, H moves to a neighboring O, forming OH• group, then H_2O is formed at the surface [152].

Furthermore, after H_2S treatment, the new material could be created:

$$Cu^{2+} + H_2S \rightarrow CuS + 2\ H^{+} \qquad (24)$$

Therefore, CuS could be the beneficial byproduct of $CuO\text{-}TiO_2$ under H_2S treatment, combined with CuO, become co-catalyst works together in the material. By

consequence, two simultaneous phenomena occur include: S-doped TiO_2 and CuS-CuO-TiO_2 dual co-catalyst, as result, the photocatalytic activity of the material was improved under solar light irradiation. **Table 3.3** presents the result of the photodegradation of methanol in aqueous solution under solar light irradiation. The improvement of methanol degradation (58.5%) in the presence of H_2S treatment is the strong evidence of the existence of another co-catalyst in the material.

Table 3.3: Decomposition of methanol using CuO/TiO_2 with/without H_2S treatment.

Sample	% decomposition
CuO/TiO_2 3 wt.%	50.8
CuO/TiO_2 3 wt.% with H_2S treatment	58.5

General conclusions and recommendations

The main purpose of this research thesis was to prepare efficient TiO_2-based photocatalysts for decomposition of organic compounds. The key approach was to develop materials possessing strong light absorption for photocatalytic reactions. To that end, three main strategies were chosen: modifying the structure of semiconductors or controlling the morphology of TiO_2, coupling with other metals (Cu, Ni, Pt) as co-catalysts and doping TiO_2 with a non-metal element (sulfur).

We started with the development of a novel oxidation co-catalysts on TiO_2-based photocatalyst. First, we synthesized and characterized TiO_2 nanoparticles (NPs) by modifying the structure of semiconductors or controlling the morphology of TiO_2 by synthesizing TNDs and then loading TNDs over SiO_2 nanospheres. This method provided the uniform in size and shape of material, with a high surface area and controlled porosity, which are of great importance for catalytic applications. Furthermore, SiO_2 nanoparticles could be easily removed by sodium hydroxide or potassium hydroxide, to provide the hollow structure of TiO_2 that adsorb more light irradiation.

Next, to study the effect of co-catalyst on TiO_2, we tested the coupling of different metals. Pt, Ni, and Cu loaded over TiO_2 NPs by ionic bonding all bring the new materials with high specific surface area. This property contributes to the improvement of charge separation and transfer characteristics towards the excellent photocatalytic performance, which resulted in efficient degradation of organic pollutants under solar irradiation. By comparing the three metals (Pt, Ni, and Cu), CuO/TiO_2 showed higher light absorption and higher degradation of methanol under the same conditions. Therefore, the use of CuO/TiO_2 in water treatment might be of interest in degradation of other organic pollutants.

We employed a novel H_2S treatment method to prepare an efficient sunlight-driven photocatalyst based on CuO/TiO_2. The S-doped CuO/TiO_2 and the produced material CuS co-exist as dual co-catalyst that enhance light absorption, charge transfer, and separation. An enhancement of photocatalytic performance of methanol degradation was also observed under solar irradiation.

The approach used in this work provided an interesting mean to prepare nanocomposite photocatalysts that could improve both solar light utilization and charge separation in degradation of organic pollutants in wastewater treatment. It is obvious that this project can be supplemented by further studies. For example, further investigate the shaped-sized effects of TiO_2 NPs on the electron-hole separation, recombination and transportation mechanism between TiO_2 and another smaller band gap energy semiconductor, in order to optimize their application in photocatalyst; further study the effect of the combination of cation - anion doped on the performance of TiO_2 and its derivatives in photocatalyst wastewater treatment; . In addition, the project was only studied on a small laboratory scale. Further research is therefore needed before the application of the new developed materials in wastewater treatment.

References

[1] S. Malato, P. Fernandez-Ibanez, M.I. Maldonado, J. Blanco, W. Gernjak, Decontamination and disinfection of water by solar photocatalysis: Recent overview and trends, Catal. Today. 147 (2009) 1–59. doi:10.1016/j.cattod.2009.06.018.

[2] T. Wintgens, F. Salehi, R. Hochstrat, T. Melin, Emerging contaminants and treatment options in water recycling for indirect potable use, Water Sci. Technol. 57 (2008) 99–107. doi:10.2166/wst.2008.799.

[3] S.D. Richardson, Environmental mass spectrometry: Emerging contaminants and current issues, Anal. Chem. 84 (2012) 747–778. doi:10.1021/ac202903d.

[4] W. Atul, G. Gaikward, M. Dondhe, N. Khaty, Removal of organic pollutant from water by heterogeneous photocatalysis: A review, Res. J. Chem. Environ. 17 (2013) 84–94.

[5] R. Perez, M. Perez, A fundamental look at energy reserves for the planet, Int. Energy Agency SHCP Sol. Updat. 50 (2009) 2–3.

[6] P.T. Anastas, J.C. Warner, Green Chemistry: Theory and Practice, Oxford University Press, 1998. https://books.google.ca/books?id=SrO8QgAACAAJ.

[7] N. Muller, B. Nowack, J. Saari, Environment: Photocatalysis for water treatment, Obs. Brief. No. 2. August (2010) 1–4.

[8] L. Brand, C.-S. Ciesla, M. Werner, Chemistry & Materials: Applications of photocatalysis, Obs. Brief. No. 10. February (2011) 1–4.

[9] A. Fujishima, K. Honda, Electrochemical photolysis of water at a semiconductor electrode, Nature. 238 (1972) 37–38. doi:10.1038/238037a0.

[10] A. Kołodziejczak-Radzimska, T. Jesionowski, Zinc Oxide - From synthesis to application: A review, Materials (Basel). 7 (2014) 2833–2881.

doi:10.3390/ma7042833.

[11] M. Mishra, D.-M. Chun, α-Fe_2O_3 as a photocatalytic material: A review, Appl. Catal. A Gen. 498 (2015) 126–141. doi:10.1016/j.apcata.2015.03.023.

[12] L. Cheng, Q. Xiang, Y. Liao, H. Zhang, CdS-Based photocatalysts, Energy Environ. Sci. 11 (2018) 1362–1391. doi:10.1039/C7EE03640J.

[13] N. Kaur, S. Kaur, J. Singh, M. Rawat, A review on Zinc Sulphide nanoparticles: From synthesis, properties to applications, J. Bioelectron. Nanotechnol. 1 (2016) 1–5. doi:10.13188/2475-224x.1000006.

[14] S. Chaturvedi, P. Dave, Environmental application of photocatalysis, Mater. Sci. Forum. 734 (2012) 273–294. doi:10.4028/www.scientific.net/MSF.734.273.

[15] R. Daghrir, P. Drogui, D. Robert, Modified TiO_2 for environmental photocatalytic applications: A review, Ind. Eng. Chem. Res. 52 (2013) 3581−3599. doi:10.1021/ie303468t.

[16] I. Mahmood, S. Imadi, K. Shazadi, A. Gul, K. Hakeem, Effects of pesticides on environment, in: Plant, Soil Microbes Vol. 1 Implic. Crop Sci., 2015: pp. 253–269. doi:10.1007/978-3-319-27455-3_13.

[17] F.P. Carvalho, Pesticides, environment, and food Safety, Food Energy Secur. 6 (2017) 48–60. doi:10.1002/fes3.108.

[18] A. Gusev, O. Rozovskaya, V. Shatalov, W. Aas, P. Nizzetto, Persistent organic pollutants in the environment, EMEP Status Rep. 3/2014. (2014) 1–62.

[19] K. Bull, Protocol to the 1979 Convention on Long-Range Transboundary Air Pollution on Persistent Organic Pollutants: The 1998 Agreement for the UNECE Region, in: Persistent Org. Pollut. Handb. Environ. Chem. (Vol. 3 Ser. Anthropog. Compd.), 2003: pp. 1–11. doi:10.1007/10751132_1.

[20] Secretariat of the Stockholm Convention on Persistent Organic Pollutants,

Stockholm Convention on Persistent Organic Pollutants, in: United Nations Treaty Sect., 2009: pp. 1–52. doi:10.1351/goldbook.s06019.

[21] Secretariat of the Stockholm Convention on Persistent Organic Pollutants, Stockholm Convention on Persistent Organic Pollutants, United Nations Treaty Sect. (2001) 1–19. doi:10.1017/CBO9781107415324.004.

[22] M.S. El-Shahawi, A. Hamza, A.S. Bashammakh, W.T. Al-Saggaf, An overview on the accumulation, distribution, transformations, toxicity and analytical methods for the monitoring of persistent organic pollutants, Talanta. 80 (2010) 1587–1597. doi:https://doi.org/10.1016/j.talanta.2009.09.055.

[23] M.N. Rashed, Adsorption technique for the removal of organic pollutants from water and wastewater, in: Org. Pollut. - Monit. Risk Treat. Effic., 2013: p. 28. doi:10.5772/54048.

[24] P. Kosobucki, B. Buszewski, Natural organic matter in Ecosystems - A review, Nov. Biotechnol. Chim. 13–2 (2014). doi:10.1515/nbec-2015-0002.

[25] M. Sillanpaa, Chapter 1 - General Introduction, in: Nat. Org. Matter Water - Charact. Treat. Methods, Butterworth-Heinemann, 2015: pp. 1–15. doi:https://doi.org/10.1016/B978-0-12-801503-2.00001-X.

[26] M. Sillanpaa, A. Matilainen, T. Lahtinen, Chapter 2 - Characterization of NOM, in: Nat. Org. Matter Water - Charact. Treat. Methods, Butterworth-Heinemann, 2015: pp. 17–53. doi:https://doi.org/10.1016/B978-0-12-801503-2.00002-1.

[27] J. Pickup, Environmental safety of halogenated organic by-products grom use of active chlorine, Euro Chlor Sci. Doss. 15. (2010) 1–42.

[28] W.-L. Wang, X. Zhang, Q.-Y. Wu, Y. Du, H.-Y. Hu, Degradation of natural organic matter by UV/chlorine oxidation: Molecular decomposition, formation of oxidation byproducts and cytotoxicity, Water Res. 124 (2017) 251–258. doi:https://doi.org/10.1016/j.watres.2017.07.029.

[29] K. Foxall, Chloroform Toxicological overview, CHAPD HQ, Heal. Prot. Agency. (2007) 1–12.

[30] R. Connor, WWAP, UNESCO. Director-General, The United Nations world water development report 2015: Water for a sustainable world, The United Nations Educational, Scientific and Cultural Organization, 2015.

[31] N.F. Gray, Chapter Thirty-Five - Filtration methods, in: Microbiol. Waterborne Dis. (Second Ed.) - Microbiol. Asp. Risks., Academic Press, London, 2014: pp. 631–650. doi:https://doi.org/10.1016/B978-0-12-415846-7.00035-4.

[32] C. Solomon, P. Casey, C. Mackne, A. Lake, Ultraviolet Disinfection, Environ. Technol. Initiat. (1998) 1–2. doi:10.1061/40569(2001)494.

[33] A. Gadgil, A. Drescher, D. Greene, P. Miller, C. Motau, F. Stevens, Field testing UV disinfection of drinking water, 23rd WEDC Conf. - Water Sanit. All Partnerships Innov. Durban, South Africa 1997. (1997) 394–396.

[34] W.H. Glaze, Drinking-water treatment with ozone, in: Environ. Sci. Technol., American Chemical Society, 1987: pp. 224–230. doi:10.1021/es00157a001.

[35] W.H. Glaze, J.-W. Kang, D.H. Chapin, The chemistry of water treatment processes involving ozone, hydrogen peroxide and ultraviolet radiation, Ozone Sci. Eng. 9 (1987) 335–352. doi:10.1080/01919518708552148.

[36] A. Bhatnagar, M. Sillanpaa, Removal of natural organic matter (NOM) and its constituents from water by adsorption – A review, Chemosphere. 166 (2017) 497–510. doi:10.1016/j.chemosphere.2016.09.098.

[37] O. Legrini, E. Oliveros, A.M. Braun, Photochemical processes for water treatment, Chem. Rev. 93 (1993) 671–698. doi:10.1021/cr00018a003.

[38] A. Matilainen, M. Sillanpaa, Removal of natural organic matter from drinking water by advanced oxidation processes, Chemosphere. 80 (2010) 351–365.

doi:10.1016/j.chemosphere.2010.04.067.

[39] C.P. Huang, C. Dong, Z. Tang, Advanced chemical oxidation: Its present role and potential future in hazardous waste treatment, Waste Manag. 13 (1993) 361–377. doi:https://doi.org/10.1016/0956-053X(93)90070-D.

[40] G. Tchobanoglous, F.L. Burton, H.D. Stensel, Wastewater Engineering, Treatment and Reuse, Metcalf & Eddy, Inc., McGraw-Hill Companies, Inc., 1991.

[41] Y. Deng, R. Zhao, Advanced oxidation processes (AOPs) in wastewater treatment, Curr. Pollut. Reports. 1 (2015) 167–176. doi:10.1007/s40726-015-0015-z.

[42] Z. Guo, R. Ma, G. Li, Degradation of phenol by nanomaterial TiO_2 in wastewater, Chem. Eng. J. 119 (2006) 55–59. doi:https://doi.org/10.1016/j.cej.2006.01.017.

[43] M. Kitis, S.S. Kaplan, Advanced oxidation of natural organic matter using hydrogen peroxide and iron-coated pumice particles, Chemosphere. 68 (2007) 1846–1853. doi:https://doi.org/10.1016/j.chemosphere.2007.03.027.

[44] J. Nawrocki, B. Kasprzyk-Hordern, The efficiency and mechanisms of catalytic ozonation, Appl. Catal. B Environ. 99 (2010) 27–42. doi:https://doi.org/10.1016/j.apcatb.2010.06.033.

[45] S. Nandy, A. Banerjee, E. Fortunato, R. Martins, A review on Cu_2O and Cu^{I-}based p-type wemiconducting transparent oxide materials: Promising candidates for new generation oxide based electronics, in: Rev. Adv. Sci. Eng. No. 4, American Scientific Publishers, 2013: pp. 273–304. doi:10.1166/rase.2013.1045.

[46] A. Di Paola, E. Garcia-Lopez, G. Marci, L. Palmisano, A survey of photocatalytic materials for environmental remediation, J. Hazard. Mater. 211–212 (2012) 3–29. doi:https://doi.org/10.1016/j.jhazmat.2011.11.050.

[47] M.N. Chong, B. Jin, C.W.K. Chow, C. Saint, Recent developments in photocatalytic water treatment technology: A review, Water Res. 44 (2010) 2997–3027.

doi:https://doi.org/10.1016/j.watres.2010.02.039.

[48] A. Albini, M. Fagnoni, 1908: Giacomo Ciamician and the concept of green chemistry, ChemSusChem. 1 (2008) 63–66. doi:10.1002/cssc.200700015.

[49] L. Bruner, J. Kozak, Zur kenntnis der photokatalyse. I. Die lichtreaktion in gemischen: Uransalz + Oxalsäure, Zeitschrift Für Elektrochemie Und Angew. Phys. Chemie. 17 (2018) 354–360. doi:10.1002/bbpc.19110170905.

[50] A. Fujishima, K. Honda, Electrochemical photolysis of water at a semiconductor electrode, Nature. 238 (1972) 37–38. doi:10.1038/238037a0.

[51] A. Kudo, Y. Miseki, Heterogeneous photocatalyst materials for water splitting, Chem. Soc. Rev. 38 (2009) 253–278. doi:10.1039/B800489G.

[52] K. Maeda, Photocatalytic water splitting using semiconductor particles: History and recent developments, J. Photochem. Photobiol. C Photochem. Rev. 12 (2011) 237–268. doi:10.1016/j.jphotochemrev.2011.07.001.

[53] R. Abe, Recent progress on photocatalytic and photoelectrochemical water splitting under visible light irradiation, J. Photochem. Photobiol. C Photochem. Rev. 11 (2010) 179–209. doi:10.1016/j.jphotochemrev.2011.02.003.

[54] T. Inoue, A. Fujishima, S. Konishi, K. Honda, Photoelectrocatalytic reduction of carbon dioxide in aqueous suspensions of semiconductor powders, Nature. 277 (1979) 637–638. http://dx.doi.org/10.1038/277637a0.

[55] D.B. Judd, D.L. MacAdam, G. Wyszecki, H.W. Budde, H.R. Condit, S.T. Henderson, J.L. Simonds, Spectral distribution of typical daylight as a function of correlated color temperature, J. Opt. Soc. Am. 54 (1964) 1031–1040. doi:10.1364/JOSA.54.001031.

[56] K. Maeda, K. Domen, Photocatalytic water splitting: Recent progress and future challenges, J. Phys. Chem. Lett. 1 (2010) 2655–2661. doi:10.1021/jz1007966.

[57] S. Wang, J.-H. Yun, B. Luo, T. Butburee, P. Peerakiatkhajohn, S. Thaweesak, M. Xiao, L. Wang, Recent progress on visible light responsive heterojunctions for photocatalytic applications, J. Mater. Sci. Technol. 33 (2017) 1–22. doi:https://doi.org/10.1016/j.jmst.2016.11.017.

[58] M.N. Chong, B. Jin, C.W.K. Chow, C. Saint, Recent developments in photocatalytic water treatment technology: A review, Water Res. 44 (2010) 2997–3027. doi:10.1016/j.watres.2010.02.039.

[59] O. Carp, C.L. Huismanb, A. Rellerb, Photoinduced reactivity of titanium dioxide, Prog. Solid State Chem. 32 (2004) 33–177. doi:10.1016/j.progsolidstchem.2004.08.001.

[60] M.D. Hernandez-Alonso, F. Fresno, S. Suarez, J.M. Coronado, Development of alternative photocatalysts to TiO_2: Challenges and opportunities, Energy Environ. Sci. 2 (2009) 1231–1257. doi:10.1039/B907933E.

[61] A. Navrotsky, J.C. Jamieson, O.J. Kleppa, Enthalpy of transformation of a high-pressure polymorph of titanium dioxide to the rutile modification, Science (80-.). 158 (1967) 388–389. http://science.sciencemag.org/content/158/3799/388.abstract.

[62] Q. Zhang, L. Gao, J. Guo, Effects of calcination on the photocatalytic properties of nanosized TiO_2 powders prepared by $TiCl_4$ hydrolysis, Appl. Catal. B Environ. 26 (2000) 207–215. doi:https://doi.org/10.1016/S0926-3373(00)00122-3.

[63] J. Muscat, V. Swamy, N.M. Harrison, First-principles calculations of the phase stability of TiO_2, Phys. Rev. B. 65 (2002) 224112. https://link.aps.org/doi/10.1103/PhysRevB.65.224112.

[64] K. Tanaka, M.F.V. Capule, T. Hisanaga, Effect of crystallinity of TiO_2 on its photocatalytic action, Chem. Phys. Lett. 187 (1991) 73–76. doi:10.1016/0009-2614(91)90486-S.

[65] T.L. Thompson, J.T. Yates, Surface science studies of the photoactivation of TiO_2 -

New photochemical processes, Chem. Rev. 106 (2006) 4428–4453. doi:10.1021/cr050172k.

[66] L. Wang, T. Sasaki, Y. Ebina, K. Kurashima, M. Watanabe, Fabrication of controllable ultrathin hollow shells by layer-by-layer assembly of exfoliated titania nanosheets on polymer templates, Chem. Mater. 14 (2002) 4827–4832. doi:10.1021/cm020685x.

[67] J. Zhang, Y. Wu, M. Xing, S.A.K. Leghari, S. Sajjad, Development of modified N doped TiO_2 photocatalyst with metals, nonmetals and metal oxides, Energy Environ. Sci. 3 (2010) 715–726. doi:10.1039/b927575d.

[68] K. Nakata, A. Fujishima, TiO_2 photocatalysis: Design and applications, J. Photochem. Photobiol. C Photochem. Rev. 13 (2012) 169–189. doi:10.1016/j.jphotochemrev.2012.06.001.

[69] W. Ho, J.C. Yu, S. Lee, Synthesis of hierarchical nanoporous F-doped TiO_2 spheres with visible light photocatalytic activity, Chem. Commun. (2006) 1115–1117. doi:10.1039/B515513D.

[70] C.B. Almquist, P. Biswas, Role of synthesis method and particle size of nanostructured TiO_2 on its photoactivity, J. Catal. 212 (2002) 145–156. doi:https://doi.org/10.1006/jcat.2002.3783.

[71] D. Li, Y. Xia, Fabrication of titania nanofibers by electrospinning, Nano Lett. 3 (2003) 555–560. doi:10.1021/nl034039o.

[72] T. Kasuga, M. Hiramatsu, A. Hoson, T. Sekino, K. Niihara, Formation of titanium oxide nanotube, Langmuir. 14 (1998) 3160–3163. doi:10.1021/la9713816.

[73] D. V. Bavykin, J.M. Friedrich, F.C. Walsh, Protonated titanates and TiO_2 nanostructured materials: Synthesis, properties, and applications, Adv. Mater. 18 (2006) 2807–2824. doi:10.1002/adma.200502696.

[74] A. Ghicov, P. Schmuki, Self-ordering electrochemistry: A review on growth and functionality of TiO_2 nanotubes and other self-aligned MOx structures, Chem. Commun. (2009) 2791–2808. doi:10.1039/B822726H.

[75] T. Shibata, N. Sakai, K. Fukuda, Y. Ebina, T. Sasaki, Photocatalytic properties of titania nanostructured films fabricated from titania nanosheets, Phys. Chem. Chem. Phys. 9 (2007) 2413–2420. doi:10.1039/B618448K.

[76] T. Shichi, K. Katsumata, Development of photocatalytic self-cleaning glasses utilizing metal oxide nanosheets, J. Surf. Finish. Soc. Japan. 61 (2010) 30–35. doi:10.4139/sfj.61.30.

[77] C. Hong, J. Kang, J. Lee, H. Zheng, S. Hong, D. Lee, C. Lee, Photothermal therapy using TiO_2 nanotubes in combination with near-infrared laser, J. Cancer Ther. 1 (2010) 52–58. doi:10.4236/jct.2010.12009.

[78] C.-T. Dinh, H. Yen, F. Kleitz, T.-O. Do, Three-dimensional ordered assembly of thin-shell Au/TiO_2 hollow nanospheres for enhanced visible-light-driven photocatalysis, Angew. Chemie Int. Ed. 53 (2014) 6618–6623. doi:10.1002/anie.201400966.

[79] J.G. Yu, Y.R. Su, B. Cheng, Template-free fabrication and enhanced photocatalytic activity of hierarchical macro-/mesoporous titania, Adv. Funct. Mater. 17 (2007) 1984–1990. doi:10.1002/adfm.200600933.

[80] N. Shamim, V.K. Sharma, Sustainable nanotechnology and the environment: Advances and achievements, American Chemical Society, Washington, DC, 2013. doi:10.1021/bk-2013-1124.

[81] S.M. Gupta, M. Tripathi, A review of TiO_2 nanoparticles, Chinese Sci. Bull. 56 (2011) 1639–1657. doi:10.1007/s11434-011-4476-1.

[82] S. Sonmezoglu, C. Akyurek, S. Akin, High-efficiency dye-sensitized solar cells using ferrocene-based electrolytes and natural photosensitizers, J. Phys. D. Appl.

Phys. 45 (2012) 425101. doi:10.1088/0022-3727/45/42/425101.

[83] A. Kay, M. Gratzel, Low cost photovoltaic modules based on dye sensitized nanocrystalline titanium dioxide and carbon powder, Sol. Energy Mater. Sol. Cells. 44 (1996) 99–117. doi:10.1016/0927-0248(96)00063-3.

[84] Z. Ambrus, N. Balazs, T. Alapi, G. Wittmann, P. Sipos, A. Dombi, K. Mogyorosi, Synthesis, structure and photocatalytic properties of Fe(III)-doped TiO_2 prepared from $TiCl_3$, Appl. Catal. B Environ. 81 (2008) 27–37. doi:10.1016/j.apcatb.2007.11.041.

[85] M. Subramanian, S. Vijayalakshmi, S. Venkataraj, R. Jayavel, Effect of cobalt doping on the structural and optical properties of TiO_2 films prepared by sol–gel process, Thin Solid Films. 516 (2008) 3776–3782. doi:10.1016/j.tsf.2007.06.125.

[86] L.M. Martinez T, C. Montes de Correa, J.A. Odriozola, M.A. Centeno, Synthesis and characterization of xerogel titania modified with Pd and Ni, J. Mol. Catal. A Chem. 253 (2006) 252–260. doi:10.1016/j.molcata.2006.03.052.

[87] M.M. Mohamed, I. Othman, R.M. Mohamed, Synthesis and characterization of MnO_x/TiO_2 nanoparticles for photocatalytic oxidation of indigo carmine dye, J. Photochem. Photobiol. A Chem. 191 (2007) 153–161. doi:10.1016/j.jphotochem.2007.04.017.

[88] G. Li, N.M. Dimitrijevic, L. Chen, T. Rajh, K.A. Gray, Role of surface/interfacial Cu^{2+} sites in the photocatalytic activity of coupled $CuO\text{-}TiO_2$ nanocomposites, J. Phys. Chem. C. 112 (2008) 19040–19044. doi:10.1021/jp8068392.

[89] M.K. Seery, R. George, P. Floris, S.C. Pillai, Silver doped titanium dioxide nanomaterials for enhanced visible light photocatalysis, J. Photochem. Photobiol. A Chem. 189 (2007) 258–263. doi:10.1016/j.jphotochem.2007.02.010.

[90] G. Valverde-Aguilar, J.A. Garcia-Macedo, V. Renteria-Tapia, Optical and morphological characterization of TiO_2 films doped with silver nanoparticles, in:

M.I. Stockman (Ed.), SPIE - Int. Soc. Opt. Eng. - August 2010, 2010: p. 77572Z. doi:10.1117/12.860612.

[91] H. Irie, Y. Watanabe, K. Hashimoto, Carbon-doped anatase TiO_2 powders as a visible-light sensitive photocatalyst, Chem. Lett. 32 (2003) 772–773. doi:10.1246/cl.2003.772.

[92] S.U.M. Khan, M. Al-Shahry, W.B. Ingler Jr., Efficient photochemical water splitting by a chemically modified n-TiO_2, Science (80-.). 297 (2002) 2243–2245. doi:10.1126/science.1075035.

[93] Y. Choi, T. Umebayashi, M. Yoshikawa, Fabrication and characterization of c-doped anatase TiO_2 photocatalysts, J. Mater. Sci. 39 (2004) 1837–1839. doi:10.1023/B:JMSC.0000016198.73153.31.

[94] C. Burda, Y. Lou, X. Chen, A.C.S. Samia, J. Stout, J.L. Gole, Enhanced nitrogen doping in TiO_2 nanoparticles, Nano Lett. 3 (2003) 1049–1051. doi:10.1021/nl034332o.

[95] T. Ohno, M. Akiyoshi, T. Umebayashi, K. Asai, T. Mitsui, M. Matsumura, Preparation of S-doped TiO_2 photocatalysts and their photocatalytic activities under visible light, Appl. Catal. A Gen. 265 (2004) 115–121. doi:10.1016/j.apcata.2004.01.007.

[96] C.M. Teh, A.R. Mohamed, Roles of titanium dioxide and ion-doped titanium dioxide on photocatalytic degradation of organic pollutants (phenolic compounds and dyes) in aqueous solutions: A review, J. Alloys Compd. 509 (2011) 1648–1660. doi:10.1016/j.jallcom.2010.10.181.

[97] M.S. Lee, S.-S. Hong, M. Mohseni, Synthesis of photocatalytic nanosized TiO_2–Ag particles with sol–gel method using reduction agent, J. Mol. Catal. A Chem. 242 (2005) 135–140. doi:10.1016/j.molcata.2005.07.038.

[98] J.O. Carneiro, V. Teixeira, A. Portinha, L. Dupak, A. Magalhaes, P. Coutinho, Study

of the deposition parameters and Fe-dopant effect in the photocatalytic activity of TiO_2 films prepared by dc reactive magnetron sputtering, Vacuum. 78 (2005) 37–46. doi:10.1016/j.vacuum.2004.12.012.

[99] X.Z. Li, F.B. Li, Study of Au/Au^{3+}-TiO_2 photocatalysts toward visible photooxidation for water and wastewater treatment, Environ. Sci. Technol. 35 (2001) 2381–2387. doi:10.1021/es001752w.

[100] F.B. Li, X.Z. Li, The enhancement of photodegradation efficiency using Pt–TiO_2 catalyst, Chemosphere. 48 (2002) 1103–1111. doi:10.1016/S0045-6535(02)00201-1.

[101] F. Peng, L. Cai, L. Huang, H. Yu, H. Wang, Preparation of nitrogen-doped titanium dioxide with visible-light photocatalytic activity using a facile hydrothermal method, J. Phys. Chem. Solids. 69 (2008) 1657–1664. doi:10.1016/j.jpcs.2007.12.003.

[102] Y. Ao, J. Xu, D. Fu, C. Yuan, A simple method to prepare N-doped titania hollow spheres with high photocatalytic activity under visible light, J. Hazard. Mater. 167 (2009) 413–417. doi:10.1016/j.jhazmat.2008.12.139.

[103] M.-S. Wong, W.-C. Chu, D.-S. Sun, H.-S. Huang, J.-H. Chen, P.-J. Tsai, N.-T. Lin, M.-S. Yu, S.-F. Hsu, S.-L. Wang, H.-H. Chang, Visible-light-induced bactericidal activity of a nitrogen-doped titanium photocatalyst against human pathogens, Appl. Environ. Microbiol. 72 (2006) 6111–6116. doi:10.1128/AEM.02580-05.

[104] Z. Wu, F. Dong, W. Zhao, S. Guo, Visible light induced electron transfer process over nitrogen doped TiO_2 nanocrystals prepared by oxidation of titanium nitride, J. Hazard. Mater. 157 (2008) 57–63. doi:10.1016/j.jhazmat.2007.12.079.

[105] R. Asahi, T. Morikawa, T. Ohwaki, K. Aoki, Y. Taga, Visible-light photocatalysis in nitrogen-doped titanium oxides, Science. 293 (2001) 269–271. doi:10.1126/science.1061051.

[106] K. Takeshita, A. Yamakata, T. Ishibashi, H. Onishi, K. Nishijima, T. Ohno, Transient IR absorption study of charge carriers photogenerated in sulfur-doped

TiO_2, J. Photochem. Photobiol. A Chem. 177 (2006) 269–275. doi:10.1016/j.jphotochem.2005.06.006.

[107] C. Lettmann, K. Hildenbrand, H. Kisch, W. Macyk, W.F. Maier, Visible light photodegradation of 4-chlorophenol with a coke-containing titanium dioxide photocatalyst, Appl. Catal. B Environ. 32 (2001) 215–227. doi:10.1016/S0926-3373(01)00141-2.

[108] L. Korosi, I. Dekany, Preparation and investigation of structural and photocatalytic properties of phosphate modified titanium dioxide, Colloids Surfaces A Physicochem. Eng. Asp. 280 (2006) 146–154. doi:10.1016/j.colsurfa.2006.01.052.

[109] Z. Lu, J. Xu, X. Xie, H. Wang, C. Wang, S.-Y. Kwok, T. Wong, H.L. Kwong, I. Bello, C.-S. Lee, S.-T. Lee, W. Zhang, CdS/CdSe double-sensitized zno nanocable arrays synthesized by chemical solution method and their photovoltaic applications, J. Phys. Chem. C. 116 (2012) 2656–2661. doi:10.1021/jp208254z.

[110] H. Zhang, G. Chen, D.W. Bahnemann, Photoelectrocatalytic materials for environmental applications, J. Mater. Chem. 19 (2009) 5089–5121. doi:10.1039/b821991e.

[111] R. Marschall, Semiconductor composites: strategies for enhancing charge carrier separation to improve photocatalytic activity, Adv. Funct. Mater. 24 (2014) 2421–2440. doi:10.1002/adfm.201303214.

[112] L. Samet, K. March, O. Stephan, N. Brun, F. Hosni, F. Bessousa, J. Benasseur, R. Chtourou, Radiocatalytic Cu-incorporated TiO_2 nano-particles for the degradation of organic species under gamma irradiation, J. Alloys Compd. 743 (2018) 175–186. doi:10.1016/j.jallcom.2018.02.001.

[113] M.V. Dozzi, A. Saccomanni, E. Selli, Cr(VI) photocatalytic reduction: Effects of simultaneous organics oxidation and of gold nanoparticles photodeposition on TiO_2, J. Hazard. Mater. 211–212 (2012) 188–195. doi:10.1016/j.jhazmat.2011.09.038.

[114] W.-T. Chen, V. Jovic, D. Sun-Waterhouse, H. Idriss, G.I.N. Waterhouse, The role of CuO in promoting photocatalytic hydrogen production over TiO_2, Int. J. Hydrogen Energy. 38 (2013) 15036–15048. doi:10.1016/j.ijhydene.2013.09.101.

[115] W.R. Siah, H.O. Lintang, M. Shamsuddin, H. Yoshida, L. Yuliati, Masking effect of copper oxides photodeposited on titanium dioxide: exploring UV, visible, and solar light activity, Catal. Sci. Technol. 6 (2016) 5079–5087. doi:10.1039/C6CY00074F.

[116] Q. Hu, J. Huang, G. Li, J. Chen, Z. Zhang, Z. Deng, Y. Jiang, W. Guo, Y. Cao, Effective water splitting using CuOx/TiO_2composite films: Role of Cu species and content in hydrogen generation, Appl. Surf. Sci. 369 (2016) 201–206. doi:10.1016/j.apsusc.2016.01.281.

[117] Q. Hu, J. Huang, G. Li, Y. Jiang, H. Lan, W. Guo, Y. Cao, Origin of the improved photocatalytic activity of Cu incorporated TiO_2 for hydrogen generation from water, Appl. Surf. Sci. 382 (2016) 170–177. doi:10.1016/j.apsusc.2016.04.126.

[118] Z. Li, Y. Qu, G. He, M. Humayun, S. Chen, L. Jing, Enhanced visible-light activities for PEC water reduction of CuO nanoplates by coupling with anatase TiO_2 and mechanism, Appl. Surf. Sci. 351 (2015) 681–685. doi:10.1016/j.apsusc.2015.05.190.

[119] R.M. Asmussen, M. Tian, A. Chen, A new approach to wastewater remediation based on bifunctional electrodes, Environ. Sci. Technol. 43 (2009) 5100–5105. doi:10.1021/es900582m.

[120] N.M. Mahmoodi, M. Arami, Degradation and toxicity reduction of textile wastewater using immobilized titania nanophotocatalysis, J. Photochem. Photobiol. B Biol. 94 (2009) 20–24. doi:10.1016/j.jphotobiol.2008.09.004.

[121] R. Ali, S.H. Hassan, Degradation studies on paraquat and malathion using TiO_2/ZnO based photocatalyst, Malaysian J. Anal. Sci. 12 (2008) 77–87.

[122] K. Dai, T. Peng, H. Chen, R. Zhang, Y. Zhang, Photocatalytic degradation and mineralization of commercial methamidophos in aqueous titania suspension,

Environ. Sci. Technol. 42 (2008) 1505–1510. doi:10.1021/es702268p.

[123] I.K. Konstantinou, T.M. Sakellarides, V.A. Sakkas, T.A. Albanis, Photocatalytic degradation of selected s-triazine herbicides and organophosphorus insecticides over aqueous TiO_2 suspensions, Environ. Sci. Technol. 35 (2001) 398–405. doi:10.1021/es001271c.

[124] S. Parra, J. Olivero, C. Pulgarin, Relationships between physicochemical properties and photoreactivity of four biorecalcitrant phenylurea herbicides in aqueous TiO_2 suspension, Appl. Catal. B Environ. 36 (2002) 75–85. doi:10.1016/S0926-3373(01)00283-1.

[125] E. Vulliet, C. Emmelin, J.-M. Chovelon, C. Guillard, J.-M. Herrmann, Photocatalytic degradation of sulfonylurea herbicides in aqueous TiO_2, Appl. Catal. B Environ. 38 (2002) 127–137. doi:10.1016/S0926-3373(02)00035-8.

[126] C.-T. Dinh, Y. Seo, T.-D. Nguyen, F. Kleitz, T.-O. Do, Controlled synthesis of titanate nanodisks as versatile building blocks for the design of hybrid nanostructures, Angew. Chemie Int. Ed. 51 (2012) 6608–6612. doi:10.1002/anie.201202046.

[127] W. Stober, A. Fink, E. Bohn, Controlled growth of monodisperse silica spheres in the micron size range, J. Colloid Interface Sci. 26 (1968) 62–69. doi:10.1016/0021-9797(68)90272-5.

[128] R.K. Iler, Multilayers of colloidal particles, J. Colloid Interface Sci. 21 (1966) 569–594. doi:10.1016/0095-8522(66)90018-3.

[129] D. Dambournet, I. Belharouak, K. Amine, Tailored preparation methods of TiO_2 anatase, rutile, brookite: Mechanism of formation and electrochemical properties, Chem. Mater. 22 (2010) 1173–1179. doi:10.1021/cm902613h.

[130] S. Brunauer, P.H. Emmett, E. Teller, Adsorption of gases in multimolecular layers, J. Am. Chem. Soc. 60 (1938) 309–319. doi:10.1021/ja01269a023.

[131] W.E. Acree, Basic gas chromatography (McNair, Harold M.; Miller, James M.), J. Chem. Educ. 75 (1998) 1094. doi:10.1021/ed075p1094.

[132] D. Koziej, F. Fischer, N. Kränzlin, W.R. Caseri, M. Niederberger, Nonaqueous TiO_2 nanoparticle synthesis: a versatile basis for the fabrication of self-supporting, transparent, and UV-absorbing composite films, ACS Appl. Mater. Interfaces. 1 (2009) 1097–1104. doi:10.1021/am9000584.

[133] M. Niederberger, M.H. Bartl, G.D. Stucky, Benzyl alcohol and transition metal chlorides as a versatile reaction system for the nonaqueous and low-temperature synthesis of crystalline nano-objects with controlled dimensionality, J. Am. Chem. Soc. 124 (2002) 13642–13643. doi:10.1021/ja027115i.

[134] H.N. Azlina, J.N. Hasnidawani, H. Norita, S.N. Surip, Synthesis of SiO_2 nanostructures using sol-gel method, Acta Phys. Pol. A. 129 (2016) 842–844. doi:10.12693/APhysPolA.129.842.

[135] A. Rahnama, M. Gharagozlou, Preparation and properties of semiconductor CuO nanoparticles via a simple precipitation method at different reaction temperatures, Opt. Quantum Electron. 44 (2012) 313–322. doi:10.1007/s11082-011-9540-1.

[136] Y. Li, B. Wang, S. Liu, X. Duan, Z. Hu, Synthesis and characterization of Cu_2O/TiO_2 photocatalysts for H_2 evolution from aqueous solution with different scavengers, Appl. Surf. Sci. 324 (2015) 736–744. doi:10.1016/j.apsusc.2014.11.027.

[137] H. Dang, X. Dong, Y. Dong, Y. Zhang, S. Hampshire, TiO_2 nanotubes coupled with nano-$Cu(OH)_2$ for highly efficient photocatalytic hydrogen production, Int. J. Hydrogen Energy. 38 (2013) 2126–2135. doi:10.1016/j.ijhydene.2012.11.135.

[138] H. CHOI, M. KANG, Hydrogen production from methanol/water decomposition in a liquid photosystem using the anatase structure of Cu loaded TiO_2, Int. J. Hydrogen Energy. 32 (2007) 3841–3848. doi:10.1016/j.ijhydene.2007.05.011.

[139] G. Elango, S.M. Roopan, K.I. Dhamodaran, K. Elumalai, N.A. Al-Dhabi, M.V.

Arasu, Spectroscopic investigation of biosynthesized nickel nanoparticles and its larvicidal, pesticidal activities, J. Photochem. Photobiol. B Biol. 162 (2016) 162–167. doi:10.1016/j.jphotobiol.2016.06.045.

[140] F.A.A. Rajathi, Phytofabrication of nano-crystalline platinum particles by leaves of Cerbera manghas and its antibacterial efficacy, Int. J. Pharma Bio Sci. 5 (2014) 619–628.

[141] M. Anpo, M. Takeuchi, The design and development of highly reactive titanium oxide photocatalysts operating under visible light irradiation, J. Catal. 216 (2003) 505–516. doi:10.1016/S0021-9517(02)00104-5.

[142] A. Yamakata, T. Ishibashi, H. Onishi, Kinetics of the photocatalytic water-splitting reaction on TiO_2 and Pt/TiO_2 studied by time-resolved infrared absorption spectroscopy, J. Mol. Catal. A Chem. 199 (2003) 85–94. doi:10.1016/S1381-1169(03)00021-9.

[143] B. Sun, P.G. Smirniotis, P. Boolchand, Visible light photocatalysis with platinized rutile TiO_2 for aqueous organic oxidation, Langmuir. 21 (2005) 11397–11403. doi:10.1021/la051262n.

[144] M.C. Blount, J.A. Buchholz, J.L. Falconer, Photocatalytic decomposition of aliphatic alcohols, acids, and esters, J. Catal. 197 (2001) 303–314. doi:10.1006/jcat.2000.3093.

[145] L. Cao, Z. Gao, S.L. Suib, T.N. Obee, S.O. Hay, J.D. Freihaut, Photocatalytic oxidation of toluene on nanoscale TiO_2 catalysts: Studies of deactivation and regeneration, J. Catal. 196 (2000) 253–261. doi:10.1006/jcat.2000.3050.

[146] C. Wang, R. Pagel, J.K. Dohrmann, D.W. Bahnemann, Antenna mechanism and deaggregation concept: Novel mechanistic principles for photocatalysis, Comptes Rendus Chim. 9 (2006) 761–773. doi:10.1016/j.crci.2005.02.053.

[147] T. Chen, Z. Feng, G. Wu, J. Shi, G. Ma, P. Ying, C. Li, Mechanistic studies of

photocatalytic reaction of methanol for hydrogen production on Pt/TiO_2 by in situ Fourier transform IR and time-resolved IR spectroscopy, J. Phys. Chem. C. 111 (2007) 8005–8014. doi:10.1021/jp071022b.

[148] W. Ho, J.C. Yu, S. Lee, Low-temperature hydrothermal synthesis of S-doped TiO_2 with visible light photocatalytic activity, J. Solid State Chem. 179 (2006) 1171–1176. doi:10.1016/j.jssc.2006.01.009.

[149] N. Li, X. Zhang, W. Zhou, Z. Liu, G. Xie, Y. Wang, Y. Du, High quality sulfur-doped titanium dioxide nanocatalysts with visible light photocatalytic activity from non-hydrolytic thermolysis synthesis, Inorg. Chem. Front. 1 (2014) 521–525. doi:10.1039/C4QI00027G.

[150] X. Chen, C. Burda, The electronic origin of the visible-light absorption properties of C-, N- and S-doped TiO_2 nanomaterials, J. Am. Chem. Soc. 130 (2008) 5018–5019. doi:10.1021/ja711023z.

[151] O. Diwald, T.L. Thompson, T. Zubkov, S.D. Walck, J.T. Yates, Photochemical activity of nitrogen-doped rutile TiO_2(110) in visible light, J. Phys. Chem. B. 108 (2004) 6004–6008. doi:10.1021/jp031267y.

[152] A. Davydov, K.T. Chuang, A.R. Sanger, Mechanism of H_2S oxidation by ferric oxide and hydroxide surfaces, J. Phys. Chem. B. 102 (1998) 4745–4752. doi:10.1021/jp980361p.